



Evaluation of bottom ash slagging risk during combustion of herbaceous and woody biomass fuels in a small-scale boiler by principal component analysis

Thomas Zeng¹ · Agata Mlonka-Mędrala² · Volker Lenz¹ · Michael Nelles^{1,3}

Received: 11 June 2019 / Revised: 26 July 2019 / Accepted: 26 July 2019 / Published online: 16 August 2019
© Springer-Verlag GmbH Germany, part of Springer Nature 2019

Abstract

In the short- and mid-term perspective, drastic measures for the reduction of anthropogenic emissions including extensive decarbonization of the residential and industrial heating sector have to be implemented. To replace fossil fuels, solid biogenic residues and wastes will have to be increasingly utilized. Compared to clean woody biomass, these biomass assortments are commonly characterized by higher Si and alkaline metal contents recognized as major driver for low ash melting temperatures resulting in elevated risk of bottom ash slagging. To facilitate the prediction of bottom ash slagging during combustion, several fuel indices have been proposed. Based on empirical correlations with parameters relevant for slagging behavior, e.g., ash melting temperatures or slag fraction of the bottom ash, these fuel indices were subsequently enhanced and adapted for an increasing range of biomass fuel characteristics. In this study, analysis data of 26 woody and non-woody fuels and experimental data derived from two combustion test campaigns with an automatically stoked small-scale boiler were investigated through principal component analysis. Thus, the complex interdependencies between the fuel composition and the resulting bottom ash characteristics and the applicability of existing fuel indices were evaluated. The chemometric analysis highlighted that Si, Ca, K, Mg, and also the remaining Al and S in the bottom ash are crucial fuel components in the context of bottom ash melting. On this basis, the molar ratio $(Si + P + K)/(Ca + Mg)$ was adapted and correlated with the susceptibility to slag formation which is a new parameter derived from ash content, slag fraction > 16 mm in the bottom ash, and slag category. Thus, the applicability of a newly developed fuel index was evaluated with respect to the bottom ash slagging risk during real-scale combustion. Three ranges were distinguished for the fuel index corresponding to a specific susceptibility to slag formation (i.e., low < 20 mol/g for woody biomass, elevated between 20 and 75 mol/g, and serious > 75 mol/g for straw-like fuels and blends with wood). The linear regression of the fuel index with susceptibility to slag formation exhibits a high coefficient of determination (i.e., 0.99 for woody biomass and 0.84 for straw-like fuels and their blends with wood).

Keywords Fuel index · Biomass · Combustion · Principal component analysis · Ash · Slagging · Chemometric analysis

Highlights

- Experimental data derived from combustion tests of 26 woody and non-woody biomass fuels in a small-scale boiler was analyzed.
- Principle component analysis (PCA) was applied to elucidate interdependencies between ash components and to identify most influencing ash components for slag formation.
- A new parameter for the description of bottom ash slagging is proposed.
- An adapted fuel index for the estimation of bottom ash slagging is suggested.

Electronic supplementary material The online version of this article (<https://doi.org/10.1007/s13399-019-00494-2>) contains supplementary material, which is available to authorized users.

✉ Thomas Zeng
thomas.zeng@dbfz.de

¹ DBFZ Deutsches Biomasseforschungszentrum gemeinnützige GmbH (DBFZ), Torgauer Straße 116, 04347 Leipzig, Germany

² Faculty of Energy and Fuels, AGH University of Science and Technology, Mickiewicza 30, 30059 Krakow, Poland

³ Faculty of Agricultural and Environmental Sciences, Chair of Waste and Resource Management, University of Rostock, Justus-von-Liebig-Weg 6, 18059 Rostock, Germany

Nomenclature

$\cos 2_i$	Squared loadings for i th variable (–)
Co	Contributions of the variables to the principal components (%)

Abbreviations

A_i	Ash content of fuel i (wt%)
A_{\max}	Maximal ash content of all investigated fuels (wt%)
A_N	Normalized ash content (–)
B/A	Base-to-acid ratio
BAFS	Bottom ash fraction that forms slag
BAI	Bed agglomeration index
d.b.	Dry basis
DIN	Deutsches Institut für Normung e.V. (German Institute for Standardization)
DT	Ash deformation temperature (°C)
E	Processed wood chips (i.e., end product)
EN	European standard
EN $plus$	EN $plus$ is an international acknowledged wood pellet certification scheme which was established in 2011. EN $plus$ introduced quality classes and stronger requirements to those set by the European and international product standards for solid biofuels
FT	Ash flow temperature (°C)
Fu	Fouling Index
HF	Hydrofluoric acid
HT	Ash hemisphere temperature (°C)
M	Miscanthus
PC	Principal component
PCA	Principal component analysis
R	Unprocessed wood chips (i.e., raw material)
R_s	Babcock index
S	Wheat straw
SA	Ratio of Si and Al oxides
SD	Standard deviation
S_i	Sinter category of fuel i (–)
S_{\max}	Maximal sinter category of all investigated fuels (–)
S_N	Normalized sinter category (–)
SF_i	Bottom ash fraction that forms slag > 16 mm of fuel i (wt%)
SF_{\max}	Maximal bottom ash fraction that forms slag > 16 mm of all investigated fuels (wt%)
SF_N	Normalized bottom ash fraction that forms slag > 16 mm (–)
SSF	Susceptibility (to slag formation)
S_R	Slag viscosity index
SST	Ash shrinkage starting temperature (°C)
W	Wood sawdust

1 Introduction

Both on national and international level, ambitious climate protection targets have been agreed on [1, 2]. In Germany,

greenhouse gas emissions shall be reduced by 55% until 2030 and by 70% until 2040 with respect to the baseline derived from the year 1990 [2]. This requires drastic measures for reduction of anthropogenic emissions that have to be implemented in short- and mid-term perspective including substantial energy savings and replacing fossil fuels [3–5]. In Germany, for example, the energy consumption for residential heating which contributes 43.6% of total heat consumption is currently driven by natural gas (956 PJ) and mineral oil (460 PJ), while the share of renewables is comparatively low (317 PJ) [6]. To replace fossil fuels for small-scale heating, especially solid biogenic residues and wastes have to be utilized [7, 8]. The unused technical potential of low quality woody biomass residues from forestry as well as from cereal straw in Germany has been estimated to provide an accumulated mass between 16.3 and 36.3 million t (dry matter) [9]. Compared to clean woody biomass (i.e., sawdust), these low quality biomass assortments are commonly characterized by elevated N, S, and Cl contents and high levels of Si and alkaline metals such as K that are inherent to the biomass fuel or arise from contamination with soil [10]. These elements are responsible for an elevated risk of pollutant emissions and bottom ash slagging [11], the latter being particularly critical for small-scale combustion appliances. However, ash transformation mechanisms in the context of slag formation are very complex and yet not fully understood. Accordingly, several methods have been proposed to evaluate contamination and to predict bottom ash slagging during small-scale combustion of woody and non-woody biomass. For example, the Al/200 coefficient in combination with the Fe/Mn ratio was suggested to classify wood chips as “contaminated with soil” [12]. Consequently, soil contamination is likely if both indexes exhibit values exceeding 1. Furthermore, the DAI index (i.e., the ratio between Si + Al + Fe + Ti oxides and Ca + Mg + Mn + K + P + S + Cl + Na oxides) was also proven to reflect contamination in biomass fuels for values above 0.5 [13]. Also, fuel indices for the prediction of bottom ash slagging exist providing a simplification of the complex ash transformation processes [11, 14–23]. Several of them, e.g., the base-to-acid ratio (B/A) and modifications of it (Babcock Index (R_s) and Fouling Index (Fu)), the SA index as the ratio of Si and Al oxides as well as the Slag Viscosity Index (S_R), are commonly used in the context of coal combustion [19, 20, 24–30]. Gilbe et al. evaluated slag formation during biomass combustion using the value Si-(Cl + Ca + Mg) (specified in mol/100 g ash) and validated the results by using the fraction of fuel ash that formed slag [18]. Knudsen et al. studied in detail the interaction of Si, K, and alkaline earth metals for various fuel assortments emphasizing that the molar ratios of Si/K and (Ca + Mg)/Si can provide a good indication about bottom ash slagging during combustion processes [14]. Lindström et al. suggested the reversed molar Si/(Ca + Mg) ratio as slagging index, where higher values represent increased tendency

for slag formation [31]. For phosphorus-rich fuels, an extended slagging index $(\text{Si} + \text{P} + \text{K})/(\text{Ca} + \text{Mg})$ has been proposed by Sommersacher et al. [15, 32]. For the prediction and interpretation of ash-related problems, the usefulness of ternary phase diagrams incorporating information on phase transition and melting temperatures originating either from empirical findings or from thermodynamic equilibrium calculations has been demonstrated in several studies [11, 31–36]. However, thermodynamic data is still lacking for critical biomass ash systems and still needs experimental investigations [34, 35]. In the work of Sommersacher et al. many of these fuel indices were evaluated regarding their applicability by measurements performed in lab- and real-scale combustion systems for a variety of pure biomass fuels [15]. The applicability of these fuel indices was further verified for the combustion of wood/kaolin and straw/kaolin as well as Miscanthus/peat blends [32, 37], for blended biomass pellets [38, 39] and treated wood chip assortments [40–42]. Recently, Näzelius et al. evaluated the applicability of existing indices for slagging of phosphorus-poor biomass fuels during fixed bed combustion. Based on two-tailed *t* tests, potential significant differences in fuel ash composition and ash content were identified and prediction tools, i.e., two separate triangular diagrams with $\text{K}_2\text{O}+(\text{Na}_2\text{O})$, $\text{CaO}+(\text{MgO})$, and SiO_2 as components were developed [43]. While the first diagram can be used to predict the fraction of fuel ash that forms slag, the second one predicts the sintering category of the formed slag. Very recently, Fernandez et al. presented the disintegration (i.e., by visual appearance and the easiness of manual ash disintegration) and sieving method (i.e., by measurement of ash particle size distribution) providing reliable results for the prediction of bottom ash slagging [44].

Accordingly, it was shown that the fuel indices could provide a first pre-evaluation for slagging tendencies in the bottom ash. However, though useful for providing a first indication, fuel indices still have to be handled with care since the simplification also restricts the general use. Usually several indices have to be considered simultaneously and the broadening range of fuel characteristics may necessitate the adaption of indices and the integration of further elements critical for ash slagging. To enhance the understanding of the complex ash transformation mechanism and to support the refinement of existing fuel indices and approaches for the estimation of bottom ash slagging during small-scale combustion, principal component analysis (PCA) can be applied.

In the biomass research, PCA has been widely used for biomass fuel characterization and classification [45–57]. However, the applications of PCA for thermochemical biomass conversion are fairly limited. Recently, biomass gasification processes have been investigated with PCA using literature data [58–60] as well as experimental data [61–68]. Venturini et al. investigated the effect of wood pellet quality

classes according to ISO 17225-2 on the emissions (i.e., total suspended particles, CO, NO, and PAH) of a residential pellet stove using PCA analysis which revealed that the effect of the pellet quality on the emissions is stronger than the typical operating conditions of the stove [69]. Only very few publications covered slagging during combustion. Jeguirim et al. [70] experimentally investigated the ash characteristics of phosphorus-rich biomass assortments such as grape marc, tomato waste, exhausted olive mill solid waste, and olive mill wastewater during the combustion in a small-scale boiler. As part of their study, PCA was performed to identify to which extent mineral content correlates with PM and bottom ash characteristics. A strong correlation between the $(\text{Si} + \text{K})$ molar fraction and bottom ash particles with a diameter $> 500 \mu\text{m}$ was found. Schwabl et al. investigated severity of bottom ash slagging during combustion of 14 woody and non-woody biomass assortments with respect to boiler operation (i.e., cleaning intervals, boiler load and combustion temperature, etc.) using PCA but did not include compositional data of the bottom ash [71].

In this paper, analysis data of 26 woody and non-woody biomass fuels and experimental data derived from two combustion test campaigns with an automatically stoked small-scale boiler was analyzed by PCA to identify the most influencing factors for the observed bottom ash slagging tendencies. Furthermore, applicability of existing fuel indices for the prediction of slag formation were evaluated to allow boiler operators a simple estimation of bottom ash slagging in practice.

2 Materials and methods

2.1 Fuels

Wood sawdust (W), wheat straw (S), and Miscanthus (M) were applied to produce blended biomass pellets (fuels denoted with I to X, Table 1). The wood sawdust was delivered from a commercial pellet company located in Germany. The energy crop Miscanthus (*Miscanthus × Giganteus*) was grown on a post-mining area, collected with a forage harvester and purchased as chopped material (length approx. 30 mm) from Agrarproduktion Elsteraue GmbH & Co. KG, Zwenkau in Saxony/Germany. Wheat straw bales were purchased from Agrarhandel & Transport GmbH, Schafstädt in Saxony-Anhalt/Germany. Three pure and seven binary blended biomass pellet batches were produced by PTG Pelletier- und Transportgesellschaft GmbH, Apolda in Thuringia/Germany in an industrial ring die pellet press with a nominal capacity of 1 t/h. Each batch had a weight of approx. 500 kg. For fuels denoted with XI to XXV, locally available forest residue wood chip assortments were subjected

Table 1 Overview of the applied pure and blended fuels (ratios of raw materials are given in wt%) and six case studies

Object	Test campaign	Reference	Fuel labelling	Fuel type	Description
I	1	[38, 39]	100W	Pellet	100 wt% wood sawdust
II			70W30M	Pellet	70 wt% sawdust, 30 wt% Miscanthus
III			50W50M	Pellet	50 wt% sawdust, 50 wt% Miscanthus
IV			30W70M	Pellet	30 wt% sawdust, 70 wt% Miscanthus
V			100M	Pellet	100 wt% Miscanthus
VI			70M30S	Pellet	70 wt% Miscanthus, 30 wt% wheat straw
VII			50M50S	Pellet	50 wt% Miscanthus, 50 wt% wheat straw
VIII			100S	Pellet	100 wt% wheat straw
IX			50W50S	Pellet	50 wt% sawdust, 50 wt% wheat straw
X			70W30S	Pellet	70 wt% sawdust, 30 wt% wheat straw
XI	2	[40, 42]	1-R	Wood chip	untreated fresh wood chips (coniferous residues)
XII			1-E	Wood chip	pretreated with star screen - rolling bed dryer - jigger screen
XIII			2-R	Wood chip	untreated fresh wood chips (coniferous residues)
XIV			2-E1	Wood chip	pretreated with star screen - container dryer
XV			2-E2	Wood chip	pretreated with container dryer - star screen
XVI			3-R2	Wood chip	pre-dried wood chips (coniferous residues, five month, fleece cover)
XVII			3-E2	Wood chip	pretreated with drum screening
XVIII			4-R	Wood chip	untreated fresh wood chips (coniferous residues)
XIX			4-E	Wood chip	pretreated with walking floor dryer
XX			5-R2	Wood chip	pre-dried wood chips (deciduous residues, five month, fleece cover)
XXI			5-E2	Wood chip	pretreated with pile drying – star screen
XXII			5-E3	Wood chip	pretreated with pile drying of pre-dried wood chips
XXIII			6-R	Wood chip	untreated fresh wood chips (coniferous residues)
XXIV			6-E2	Wood chip	pretreated with jigger screen - belt dryer
XXV			6-E1	Wood chip	pretreated with drum screen
XXVI			Ref	Pellet	ENplus wood pellet, class A1

to different combinations of drying and sieving technologies (Table 1). All fuels were derived from German biomass terminals in southern Bavaria except for XX to XXII which were purchased from the east of North Rhine-Westphalia. Thus, six case studies were performed which were described in detail previously by Kuptz et al. [42]. In case studies 1, 2, 4, and 6, one raw material (R) was used for both combinations of drying and sieving, while for case studies 3 and 5, two different raw materials (R1 and R2) had been used for fuel processing. For each case study, a full container load of approx. 30 m³ of wood chips was processed. As reference, commercially available ENplus wood pellets (i.e., object XXVI) were also applied for combustion tests in test campaign 2 [72].

2.2 Combustion tests

The combustion tests were performed in two test campaigns (campaign 1 [38, 39] and campaign 2 [40, 42]), and results of these studies have been published previously. The experiments were conducted in a commercially available boiler

dedicated for the combustion of wood pellets, wood chips, Miscanthus, and cereal grains with a nominal heat capacity of 30 kW (if used for wood pellet combustion). The heat output can be modulated in the range between 30 and 100% of the nominal heat capacity. The biomass fuel is conveyed via a feed auger into the combustion chamber where a moving step grate ensures the transport of fuel and bottom ash which eventually is collected in the ash pan. With a lambda probe, the oxygen content can be determined in order to guarantee optimal air-fuel ratio enabling complete combustion. A speed controlled chimney fan supplies the combustion air to the boiler and thus regulates the primary and secondary air supply. The combustion air ratio can be manually adjusted by a baffle to direct the primary combustion air to the moving grate and the secondary combustion air to the post-combustion chamber. Heat exchange was realized using a jacket-and-tube heat exchanger which was cleaned automatically by moving turbulators. The boiler was equipped with temperature measurement devices (type K, NiCr-Ni) in the fuel bed and in the secondary combustion chamber. Fuel bed temperatures were on average below 1000 °C (i.e., 907 °C ± 88 K SD) for all

combustion experiments [38, 39, 42]. For each combustion test, the boiler was operated at full load and adjusted according to the specific requirements of the employed fuels aiming for (i) low CO emissions, (ii) minimized slag formation in the bottom ash, and (iii) sufficient ash removal into the ash pan. To fulfill these requirements, adjustments of the primary and secondary combustion air supply, oxygen set value in the flue gas, and operation of the grate were necessary.

2.3 Analysis methods

Fuel analysis, sampling, and sample preparation were performed in accordance with European standards for solid biofuels [73–75]. The following parameters were analyzed: moisture, ash content, ash melting behavior (SST, DT, HT, and FT), total content of S and Cl, major elements (i.e., Al, Ca, Mg, P, K, Si, Fe, Ti, Mn, and Na), and minor elements (i.e., Cd, Cr, Cu, Pb, and Zn). The samples were digested in HF solution and then analyzed by ICP-OES. Furthermore, the whole bottom ash was gathered after the combustion test and analyzed in order to estimate the sintering degree in bottom ash corresponding to each fuel. Thus, the complete recovered ash samples from the combustion tests were sieved with a circular mesh with round holes (< 63 mm, < 45 mm, and < 16 mm), and the share of each bottom ash fraction was quantified as weight percentage of the total amount of bottom ash collected and evaluated regarding their sintering degree (i.e., bottom ash fraction that forms slag, BAFS) using a method previously developed by Öhman et al. [23]. Afterwards, the complete bottom ash samples were grinded and homogenized for analyses of major and minor elements according to the European standards for solid biofuels as above [75]. Cl was determined in the eluate of the bottom ash according to DIN EN 12457-4 [76]. Fuel ash analyses were additionally performed on fuel samples ashed at 550 °C using the same analysis methods as above. Release rates of K, Na, S, and Cl were determined according to Sommersacher et al. [15]. The fuel indices calculated within this work are listed in Table 2.

2.4 Principal component analysis

Among all chemometric analysis techniques, principal component analysis (PCA) is the most commonly used method [78–81]. The main objective of the PCA is to reduce the size of large data sets to reveal hidden relationships between objects and measured variables. Usually, collected data are compiled in a matrix X , with rows corresponding to n objects (herein fuels) described by p variables (herein fuel and ash analysis data as well as fuel bed temperatures) and calculated fuel indices) in columns. PCA transforms the set of objects by an orthogonal transformation into a set of values of linearly uncorrelated variables called principal components (PCs). Thus, largest possible variance accounting for the highest

possible variability in the data set will be described. The PCA was performed in OriginPro 2019. As PCA is sensitive to the relative scaling of the original variables, all data sets were normalized prior to the analysis. For PCA analysis, objects listed in Table 1 and two data sets of variables (Table 3) were used as input. The first data set of variables used for PCA-1 included ash content (variable 1), Cl and S content in the fuel (variable 2 and 3), fuel ash analysis (variables 4–19), bottom ash analysis (variables 20–37), K, Cl, and S release to the gas phase (variables 38–40), average fuel bed temperature (variable 41) as well as characteristic ash melting temperatures (variables 42–45), and bottom ash fraction that forms slag (variables 46–49). The second data set of variables used for PCA-2 was selected to determine most suitable indices for the prediction of bottom ash slagging, i.e., characteristic ash melting temperatures (variables 42–45), bottom ash fraction that forms slag (variables 46–49), and fuel indices (variables 50–69).

There are several methods for the determination of appropriate number of PCs selected as new variables. According to Kaiser's rule, PCs with eigenvalues exceeding one should be retained. Alternatively, PCs which describe at least 75% or even 80% of the total data variance can be considered [59, 81]. Additionally, in order to interpret the significance of retained PCs in terms of the original variables, only those loadings with absolute values exceeding 90% (for PC1) and 60% (for PC2 and PC3) of the maximum coefficient (in absolute value) in each PC were considered. Contributions of the variables (in percentage) accounting for the variability to a given PC were calculated using Eq. 1.

$$Co = \frac{\cos^2 i \cdot 100}{\sum_i \cos^2 i} \quad [-] \quad (1)$$

The cut-off for the contribution of the variables to a specific PC was evaluated either (i) based on the assumption of a uniform contribution of all included variables (i.e., for 20 considered variables, the value would be $1/20 = 5\%$) or (ii) according to the average contribution of all considered variables. A variable with a contribution larger than the cutoff can be considered as important for contributing to a specific PC. Loading and score plots are the graphical interpretations of PCA presenting the relations among variables and the objects, respectively.

2.5 Input data

The input data, i.e., complete results of the fuel and bottom ash analysis, were obtained in different research projects and have been reported and discussed previously [38, 39, 42]. Selected data from those publications and additional fuel indices used for the PCA are listed in Tables 4 and 5. The results from the bottom ash analysis are listed in Table S11. To enable the

Table 2 Calculation of fuel indices used for principal component analyses (* total S in fuel is defined as volatile S)

Field of application	Index	Formula	Unit	Reference
Indices developed for biomass combustion	(K + Na)/(2S + Cl)	$\frac{K+Na}{2S+Cl}$	mol/mol	[15]
	Si/(Ca + Mg)	$\frac{Si}{Ca+Mg}$	mol/mol	[15, 31]
	(Si + P + K)/(Ca + Mg)	$\frac{Si+P+K}{Ca+Mg}$	mol/mol	[15, 32]
	Si/K	$\frac{Si}{K}$	mol/mol	[14]
	2S/Cl	$\frac{2S}{Cl}$	mol/mol	[77]
	Al/200	$\frac{Al}{200}$	g/g	[12]
	Fe/Mn	$\frac{Fe}{Mn}$	g/g	[12]
	DAI coefficient	$DAI = \frac{SiO_2+Al_2O_3+Fe_2O_3+TiO_2}{CaO+MgO+Na_2O+MnO+K_2O+P_2O_5+Cl_2O+SO_3}$	g/g	[13]
	Cl ratio	$Cl_{ratio} = \frac{Cl+K_2O+Na_2O}{SiO_2+Al_2O_3}$	g/g	[28]
	S ratio	$S_{ratio} = \frac{S_{volatile}+K_2O+Na_2O}{SiO_2+Al_2O_3}$	g/g	[28]
Bed agglomeration index	$BAI = \frac{Fe_2O_3}{Na_2O+K_2O}$	g/g	[26, 29]	
Basic to acidic compounds ratio + P	$B/A + P = \frac{Fe_2O_3+CaO+MgO+Na_2O+K_2O+P_2O_5}{SiO_2+Al_2O_3+TiO_2}$	g/g	[19, 26, 30]	
Indices developed for coal combustion	Ratio between Si and Al oxides	$SA = \frac{SiO_2}{Al_2O_3}$	g/g	[27]
	Basic to acidic compounds ratio	$B/A = \frac{Fe_2O_3+CaO+MgO+Na_2O+K_2O}{SiO_2+Al_2O_3+TiO_2}$	g/g	[29]
	Babcock index	$RS = (B/A) \cdot S$	g/g	[26]
	Fouling index	$Fu = (B/A) \cdot (Na + K + O)$	g/g	[24]
	Slag viscosity index	$S_R = SiO_2 \cdot \frac{100}{SiO_2+Fe_2O_3+CaO+MgO}$	g/g	[26, 30]

appraisal of the used data set, selected aspects are emphasized below. The employed fuels can be categorized as phosphorus poor biomass because content of phosphorus in the fuels was max. 700 mg/kg d.b. (for object V, i.e., 100M). Blending of wood with at least 30 wt% Miscanthus or wheat straw significantly lowered ash melting temperatures HT and DT compared to pure wood pellets (object I, i.e., 100W). A further increase of the share of Miscanthus or wheat straw in the fuel blends did not significantly affect DT and HT which remained below 950 °C and below 1100 °C (except for object V, i.e., 100M), respectively. For woody biomass (i.e., objects I and XI to XXVI), DT and HT exhibited temperatures exceeding 1100 °C and 1200 °C (except for objects XIII and XIV), respectively. Share of bottom ash that forms slag according to Öhman et al. [23] revealed significant differences between woody and non-woody biomass. For all woody biomass fuels (i.e., objects I and XI to XXVI), a negligible slagging indicated by high share of bottom ash that forms slag < 16 mm was observed. Bottom ashes from the combustion of wood blended with Miscanthus or wheat straw (i.e., objects II to IV, IX and X) were characterized by a share of bottom ash that forms slag between 30 and 50 wt%. Bottom ashes from the combustion of Miscanthus, wheat straw, and blends thereof (i.e., objects V to VIII) were characterized by a share of bottom ash that forms slag between 40 and 65 wt%.

Contamination of the selected fuels can be evaluated using Al/200 coefficient and Fe/Mn ratio. If values for Al/200 in combination with Fe/Mn ratio are above 1, at least some soil

contamination is present in the respective fuels. The reference fuel (wood pellets, i.e., object I and XXVI) is clearly “uncontaminated” according to both indices. Except for object V (i.e., 100M), all non-woody biomass pellets and their blends with wood are uncontaminated (i.e., objects II to X). All unprocessed wood chip batches can be attributed either to the area “contaminated” (i.e., objects XXIII and XX) or “indifferent soil contamination” (i.e., objects XVI, XIII, and XVIII). Wood chip processing resulted in all cases in both lower Al/200 coefficients and Fe/Mn ratios indicating a reduction of the contamination. Accordingly, many of the processed wood chip batches can almost be attributed as “uncontaminated” (i.e., objects XII, XV, XVII, XIX, and XXI), while for the other processed wood chip assortments, some soil contamination remained after fuel processing.

With regard to bottom ash slagging, blending of wood with herbaceous raw materials and Miscanthus with wheat straw led to increased values of the molar ratio (Si + P + K)/(Ca + Mg), i.e., potentially increased risk of bottom ash slagging. The molar ratio (Si + P + K)/(Ca + Mg) exceeded 3.3 mol/mol in all cases. For the wood chip fuels, the highest molar (Si + P + K)/(Ca + Mg) ratios were found in the unprocessed wood chips indicating an elevated risk of slagging within these fuels. Fuel processing steps such as screening reduced molar (Si + P + K)/(Ca + Mg) ratios indicating a lower risk of slagging in the bottom ash during combustion of these biofuels. However, all woody biomass assortments were characterized by a molar ratio (Si + P + K)/(Ca + Mg) below 3 mol/mol. For the

Table 3 List of variables applied for PCA

No.	Variables	Unit	Principal component analysis
1	Ash content	wt% d.b.	PCA-1
2	Cl in the fuel	mg/kg d.b.	PCA-1
3	S in the fuel	mg/kg d.b.	PCA-1
4	Al in the fuel ash	mg/kg d.b.	PCA-1
5	Pb in the fuel ash	mg/kg d.b.	PCA-1
6	Cd in the fuel ash	mg/kg d.b.	PCA-1
7	Ca in the fuel ash	mg/kg d.b.	PCA-1
8	Cr in the fuel ash	mg/kg d.b.	PCA-1
9	Fe in the fuel ash	mg/kg d.b.	PCA-1
10	K in the fuel ash	mg/kg d.b.	PCA-1
11	Cu in the fuel ash	mg/kg d.b.	PCA-1
12	Mg in the fuel ash	mg/kg d.b.	PCA-1
13	Mn in the fuel ash	mg/kg d.b.	PCA-1
14	Na in the fuel ash	mg/kg d.b.	PCA-1
15	Ni in the fuel ash	mg/kg d.b.	PCA-1
16	P in the fuel ash	mg/kg d.b.	PCA-1
17	Si in the fuel ash	mg/kg d.b.	PCA-1
18	Ti in the fuel ash	mg/kg d.b.	PCA-1
19	Zn in the fuel ash	mg/kg d.b.	PCA-1
20	Cl in the bottom ash	mg/kg d.b.	PCA-1
21	Al in the bottom ash	mg/kg d.b.	PCA-1
22	Pb in the bottom ash	mg/kg d.b.	PCA-1
23	Cd in the bottom ash	mg/kg d.b.	PCA-1
24	Ca in the bottom ash	mg/kg d.b.	PCA-1
25	Cr in the bottom ash	mg/kg d.b.	PCA-1
26	Fe in the bottom ash	mg/kg d.b.	PCA-1
27	K in the bottom ash	mg/kg d.b.	PCA-1
28	Cu in the bottom ash	mg/kg d.b.	PCA-1
29	Mg in the bottom ash	mg/kg d.b.	PCA-1
30	Mn in the bottom ash	mg/kg d.b.	PCA-1
31	Na in the bottom ash	mg/kg d.b.	PCA-1
32	Ni in the bottom ash	mg/kg d.b.	PCA-1
33	P in the bottom ash	mg/kg d.b.	PCA-1
34	S in the bottom ash	mg/kg d.b.	PCA-1
35	Si in the bottom ash	mg/kg d.b.	PCA-1
36	Ti in the bottom ash	mg/kg d.b.	PCA-1
37	Zn in the bottom ash	mg/kg d.b.	PCA-1
38	K _{release} from bottom ash	wt%	PCA-1
39	Cl _{release} from bottom ash	wt%	PCA-1
40	S _{release} from bottom ash	wt%	PCA-1
41	T _{fuel bed}	°C	PCA-1
42	Ash melting temperature (SST)	°C	PCA-1, PCA-2
43	Ash melting temperature (DT)	°C	PCA-1, PCA-2
44	Ash melting temperature (HT)	°C	PCA-1, PCA-2
45	Ash melting temperature (FT)	°C	PCA-1, PCA-2
46	BAFS > 63 mm	wt%	PCA-1, PCA-2
47	BAFS 45–63 mm	wt%	PCA-1, PCA-2
48	BAFS 16–45 mm	wt%	PCA-1, PCA-2
49	BAFS < 16 mm	wt%	PCA-1, PCA-2

Table 3 (continued)

No.	Variables	Unit	Principal component analysis
50	K in the fuel	mg/kg d.b.	PCA-2
51	(K + Na)/(2S + Cl)	mol/mol	PCA-2
52	Si/(Ca + Mg)	mol/mol	PCA-2
53	(Si + P + K)/(Ca + Mg)	mol/mol	PCA-2
54	Si/K	mol/mol	PCA-2
55	2S/Cl	mol/mol	PCA-2
56	Al/200	g/g	PCA-2
57	Fe/Mn	g/g	PCA-2
58	DAI	g/g	PCA-2
59	SA	g/g	PCA-2
60	B/A + P	g/g	PCA-2
61	B/A	g/g	PCA-2
62	BAI	g/g	PCA-2
63	Rs	g/g	PCA-2
64	Fu	g/g	PCA-2
65	SR	g/g	PCA-2
66	Cl ratio	g/g	PCA-2
67	S ratio	g/g	PCA-2
68	SST-DT range	°C	PCA-2
69	DT-HT range	°C	PCA-2

investigated fuels, a wide range between 0.4 mol/mol (object I and XXVI) and 14.6 mol/mol (object XIII) was calculated for the molar Si/K ratio (Tables 4 and 5). The herbaceous biomass pellets and their blends with wood were characterized by a molar Si/K ratio in the range of 1.1 and 1.8 mol/mol, while object V (100M) exhibited the highest value (i.e., 2.7 mol/mol). This indicates an increased retention of K in the bottom ash especially for 100M. In contrast, unprocessed wood chips were often characterized by a higher molar Si/K ratio > 5 mol/mol (except for 4-R and 5-R2, object XVIII and XX, respectively). Wood chip processing reduced molar Si/K ratio typically between 20 (for 4-E, object XIX) and 80% (for 2-E2, object XV) resulting in molar Si/K ratios below 1.5 mol/mol (except for 2-E1 and 2-E2, object XIV and XV, respectively) which indicates a facilitated K release for the processed wood chips compared to the unprocessed wood chips.

3 Results and discussion

3.1 Principal component analysis

In the case of PCA-1, five PCs describe 81.67% of the total data variance and eight PCs have eigenvalues exceeding 1 (Table S12). All eight PCs were retained using Kaiser's rule. However, PC4 described only 6.25%, PC5 only 4.94%, PC6 only 3.62%, PC7 only 3.57%, and PC8 only 2.69% of the total data variance. Therefore, the first

three PCs accounting for 70.48% of the total data variance were considered for further evaluation.

In Fig. 1, contributions of the variables to the three PCs within PCA-1 are displayed. The cut-off value calculated as the average contribution was 2.0%. Calculation of the cut-off value according to uniform contribution of the 49 variables resulted also in 2.0%. Accordingly, major ash forming elements in the fuel ash and bottom ash such as K, Ca, Mg, and Si (variables 7, 10, 12, 17, 24, 27, 29, and 35) that are particularly relevant for the ash melting behavior as well as the characteristic slagging categories (42–46, 48, and 49) are described by PC1. Interestingly, Cl and S content in the fuel (variables 2 and 3) are also contributing substantially to PC1. Some further elements like Ni, Mn, or Cu (variables 11, 13, 15, 30, and 32) are also above the cut-off value, while e.g., Al (variable 4 and 21) which has been reported to play an important role in slag formation processes remains below the cut-off value [37, 82].

Minor ash forming elements in the fuel ash and bottom ash representing P and heavy metals such as Pb, Cr, Cu, Ti, and Cd but also S in the remaining bottom ash (variables 5, 6, 8, 11, 16, 18, 22, 23, 25, 28, 32, 33, and 36) are contributing mostly to PC2. PC3 is mainly described by parameters relevant for soil and contamination such as Fe and Al (variables 4, 9, 21, and 26) and chemically treated biomass such as Ti and Cr (variables 8, 18, 25, and 36) in the fuel and bottom ash. The latter contribute with higher values to PC3 compared to PC2 (except for Cr in the bottom ash, variable 25). The K, Cl, and S release as well as $T_{\text{fuel bed}}$ (variables 38 to 41) did not

Table 4 Ash melting temperatures, slag fractions, and fuel indices of objects I (wood pellets) and II to X (Miscanthus, straw, and blended pellets)

Variable	Parameter	Unit	I	II	III	IV	V	VI	VII	VIII	IX	X
42	SST	°C	820	790	760	720	810	660	670	650	650	690
43	DT	°C	1470	990	830	820	930	790	800	770	770	790
44	HT	°C	1480	1090	1060	1050	1210	1040	1050	1050	1040	1040
45	FT	°C	1490	1110	1230	1100	1310	1120	1090	1250	1070	1130
46	BAFS > 63 mm	wt%	0	0	8	0	26	17	35	48	14	9
47	BAFS 45–63 mm	wt%	0	0	0	10	1	0	1	4	15	25
48	BAFS 16–45 mm	wt%	0	33	25	19	17	26	17	11	15	14
49	BAFS < 16 mm	wt%	100	67	67	71	56	57	47	37	56	52
50	K in the fuel	mg/kg d.b.	497	1850	3840	5270	8210	10,100	11,300	14,500	7640	5850
51	(K + Na)/(2S + Cl)	mol/mol	2.3	2.3	2.3	2.5	2.4	2.8	3.5	2.7	2.9	2.8
52	Si/(Ca + Mg)	mol/mol	0.2	1.8	3.0	3.2	8.1	4.4	4.7	4.3	4.1	3.7
53	(Si + P + K)/(Ca + Mg)	mol/mol	0.8	3.3	6.0	6.4	11.5	8.0	7.6	6.9	6.6	5.9
54	Si/K	mol/mol	0.4	1.4	1.1	1.1	2.7	1.4	1.7	1.7	1.8	1.8
55	2S/Cl	mol/mol	0.8	1.3	1.3	1.0	0.8	0.8	0.9	0.8	1.1	1.0
56	Al/200	g/g	0.1	0.7	0.6	0.7	3.2	0.7	0.7	0.6	0.4	0.4
57	Fe/Mn	g/g	0.3	0.8	0.6	0.8	1.3	0.5	0.2	0.1	0.2	0.2
58	DAI	g/g	0.2	1.0	1.1	1.0	2.0	1.3	1.3	1.3	1.4	1.3
59	SA	g/g	4.2	9.3	17	21	14	37	58	85	67	55
60	B/A + P	g/g	6.4	1.5	1.4	1.8	0.8	1.3	1.2	1.2	1.1	1.2
61	B/A	g/g	5.7	1.3	1.3	1.5	0.7	1.2	1.1	1.1	1.0	1.1
62	BAI	g/g	0.1	0.1	0.1	0.1	0.1	0.0	0.0	0.0	0.0	0.0
63	Rs	g/g	0.0	0.0	0.1	0.1	0.0	0.1	0.1	0.1	0.1	0.0
64	Fu	g/g	188	56	73	97	33	71	66	65	49	58
65	S _R	g/g	19	65	77	75	85	81	83	83	82	80
66	Cl _{ratio}	g/g	2.5	0.8	1.0	1.2	0.6	1.0	0.9	0.9	0.8	0.9
67	S _{ratio}	g/g	2.5	0.8	1.0	1.2	0.6	1.0	0.9	0.9	0.8	0.9

considerably contribute to PC1, PC2, and PC3 within PCA-1. Score and loading plots performed for PCA-1 are presented in Fig. 2.

Accordingly, score plots (left side of Fig. 2) illustrate groups of objects while loading plots (right side of Fig. 2) show the contribution of the variables to each PC. Those variables that are closest to the axes of the corresponding PC and possessing the longest vector contribute most to this PC. PC1 in PCA-1 described 41.56% of the total data variance. Two major groups might be distinguished: The first includes wood-derived samples (objects I and XI to XXVI), and the second group illustrates similarities between herbaceous biomass and fuel blends with woody biomass (objects II-X). As evident by the position close to the *x*-axis in Fig. 2 (loading plot, top) and by its positive value, the following variables contribute most to the position of woody biomass: Ca and Mg content both in the fuel and bottom ash, deformation temperature (DT), hemisphere temperature (HT), and fraction of bottom ash that forms slag (BAFS) < 16 mm (variables 7, 12, 24, 29, 43, 44, and 49). Accordingly, for fuels with wheat straw and Miscanthus (objects II to X), ash content, S and Cl content

in the fuel, and K and Si content in the fuel and bottom ash as well as fraction of bottom ash that forms slag (BAFS) > 63 mm and 16–45 mm, respectively (variables 1, 2, 3, 10, 17, 27, 35, 46, 48), were the most relevant variables for their position in score plot (Fig. 2, top). Based on PC2, describing 17.43% of the total data variance, fuel 70W30M (object II) is more similar to pure wood pellets (object I and XXVI) than to the any other investigated fuels (object III to XXV). Thus, Pb and Ti in the fuel ash as well as Cr, Cu, S, and Ti in the bottom ash (variables 5, 18, 25, 28, 34, and 36) contribute most to the position of 70W30M (object II), while concentration of Cd, Cu, Na, and Zn in the fuel ash (variables 6, 11, 14, and 19) as well as P in the bottom ash (variable 33) are most relevant for the score of pure wood pellets (object I and XXVI) in Fig. 2 (top). It is apparent that PC1 in PCA-1 is connected with the slagging behavior. The well-known slagging index (Si + P + K)/(Ca + Mg), i.e., variable 53, is also represented by the position of its elements on opposite sides of the plot origin. Al can be found in the same quadrant as Ca and Mg, though contribution is lower which is also a consequence to the high contribution of Al to PC3, which is associated with soil

Table 5 Ash melting temperatures, slag fractions, and fuel indices of objects XI to XXV (i.e., processed and unprocessed wood chips) and XXXVI (wood pellets)

Variable	Parameter	Unit	XI	XII	XIII	XIV	XV	XVI	XVII	XVIII	XIX	XX	XXI	XXII	XXIII	XXIV	XXV	XXXVI
42	SST	°C	1160	1220	1110	1070	1010	1140	980	970	1040	1120	980	1160	1210	1120	1120	680
43	DT	°C	1200	1490	1170	1140	1230	1190	1200	1220	1320	1200	1200	1330	1280	1390	1380	1440
44	HT	°C	1210	1490	1200	1160	1280	1250	1210	1240	1350	1220	1220	1390	1310	1460	1420	1450
45	FT	°C	1220	1490	1220	1170	1310	1340	1220	1260	1390	1230	1250	1420	1330	1470	1450	1460
46	BAFS > 63 mm	wt%	0	0	0	0	0	0	0	0	0	0	0	0	0	0	0	0
47	BAFS 45 mm - 63 mm	wt%	0	0	0	0	0	0	0	0	0	0	0	0	0	0	0	0
48	BAFS 16 mm - 45 mm	wt%	0	0	0	3	0	0	0	0	0	0	0	0	0	0	0	0
49	BAFS < 16 mm	wt%	100	100	100	97	100	100	100	100	100	100	100	100	100	100	100	100
50	K in the fuel	mg/kg d.b.	1318	970	1790	1449	1166	1553	1336	1431	1173	1977	1864	2493	2042	1327	1491	444
51	(K + Na)/(2S + Cl)	mol/mol	3.0	3.2	3.0	2.8	3.1	3.7	4.0	3.6	3.5	5.0	4.9	5.1	4.6	4.4	5.2	1.6
52	Si/(Ca + Mg)	mol/mol	1.3	0.3	2.6	1.7	0.8	2.2	0.6	0.7	0.5	1.0	0.7	0.5	0.7	0.3	0.4	0.2
53	(Si + P + K)/(Ca + Mg)	mol/mol	1.5	0.6	2.9	2.1	1.1	2.8	1.2	1.2	1.0	1.5	1.3	0.9	0.8	0.7	0.7	0.6
54	Si/K	mol/mol	5.5	1.1	14.6	4.8	2.7	5.0	1.2	1.6	1.2	2.6	1.5	1.4	5.0	1.1	1.3	0.4
55	2S/Cl	mol/mol	5.5	3.9	2.5	4.5	5.1	6.4	4.5	4.8	4.6	4.9	5.5	5.8	4.2	2.8	2.1	0.9
56	Al/200	g/g	2.1	0.7	8.0	2.9	1.1	2.2	1.0	1.6	1.0	2.4	1.2	2.2	8.8	1.5	2.0	0.1
57	Fe/Mn	g/g	0.5	0.2	0.7	0.3	0.2	0.5	0.3	0.3	0.3	1.1	0.5	5.8	6.3	1.4	1.5	0.2
58	DAI	g/g	0.8	0.3	1.8	1.2	0.7	0.8	0.5	0.6	0.4	0.5	0.4	0.3	1.1	0.4	0.4	0.1
59	SA	g/g	7.6	4.7	5.1	4.9	7.8	5.6	4.6	3.5	3.9	4.3	4.5	3.9	1.8	2.3	1.6	3.5
60	B/A + P	g/g	1.4	3.8	0.6	0.8	1.5	1.4	2.4	2.0	3.0	2.3	3.0	3.5	1.1	2.9	2.7	17.1
61	B/A	g/g	1.2	3.4	0.5	0.8	1.3	1.2	2.1	1.8	2.6	2.1	2.6	3.0	1.0	2.7	2.5	15.6
62	BAI	g/g	0.2	0.1	0.4	0.2	0.2	0.1	0.1	0.1	0.1	0.1	0.1	0.1	0.6	0.2	0.2	0.1
63	Rs	g/g	0.0	0.0	0.0	0.0	0.0	0.0	0.0	0.0	0.0	0.0	0.0	0.1	0.0	0.0	0.0	0.1
64	Fu	g/g	18	63	5.7	12	23	24	59	43	70	49	74	86	14	54	54	466
65	S _R	g/g	50	25	68	63	48	53	40	41	32	38	34	30	45	27	26	7.3
66	Cl _{ratio}	g/g	0.3	0.9	0.2	0.3	0.4	0.4	0.9	0.7	1.0	0.8	1.1	1.2	0.3	0.8	0.8	5.9
67	S _{ratio}	g/g	0.3	0.9	0.2	0.3	0.4	0.4	0.9	0.7	1.0	0.8	1.1	1.2	0.3	0.8	0.8	5.9

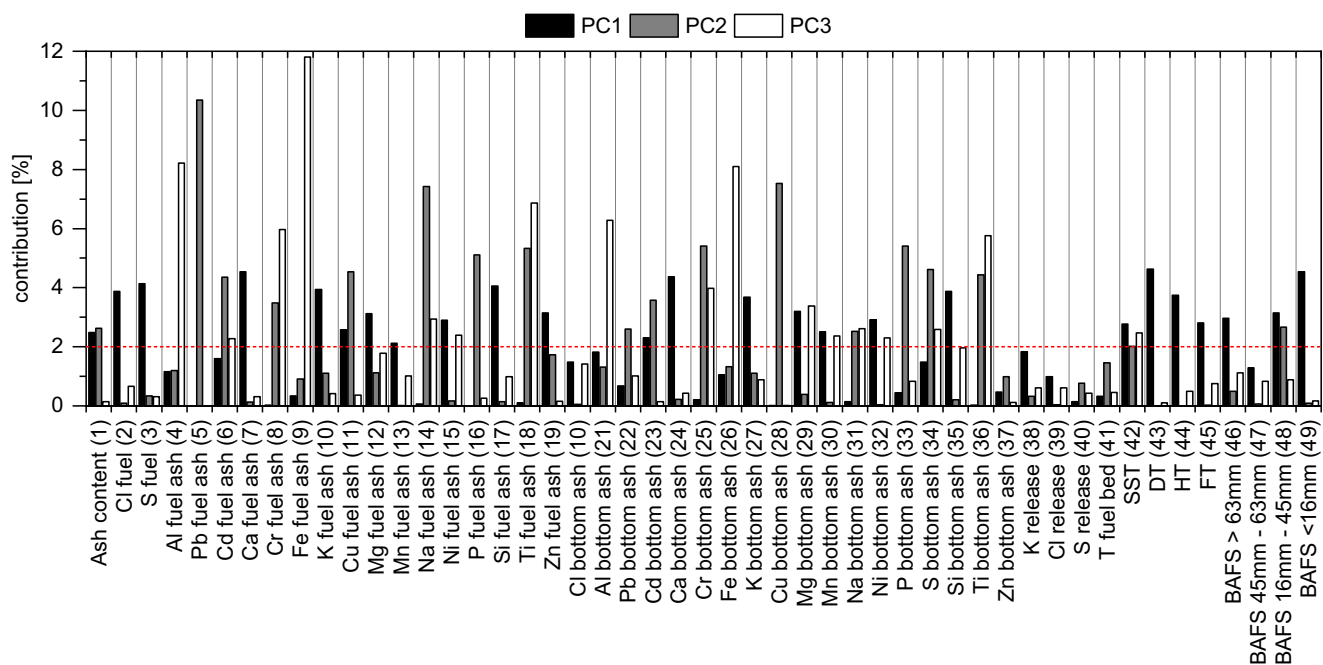
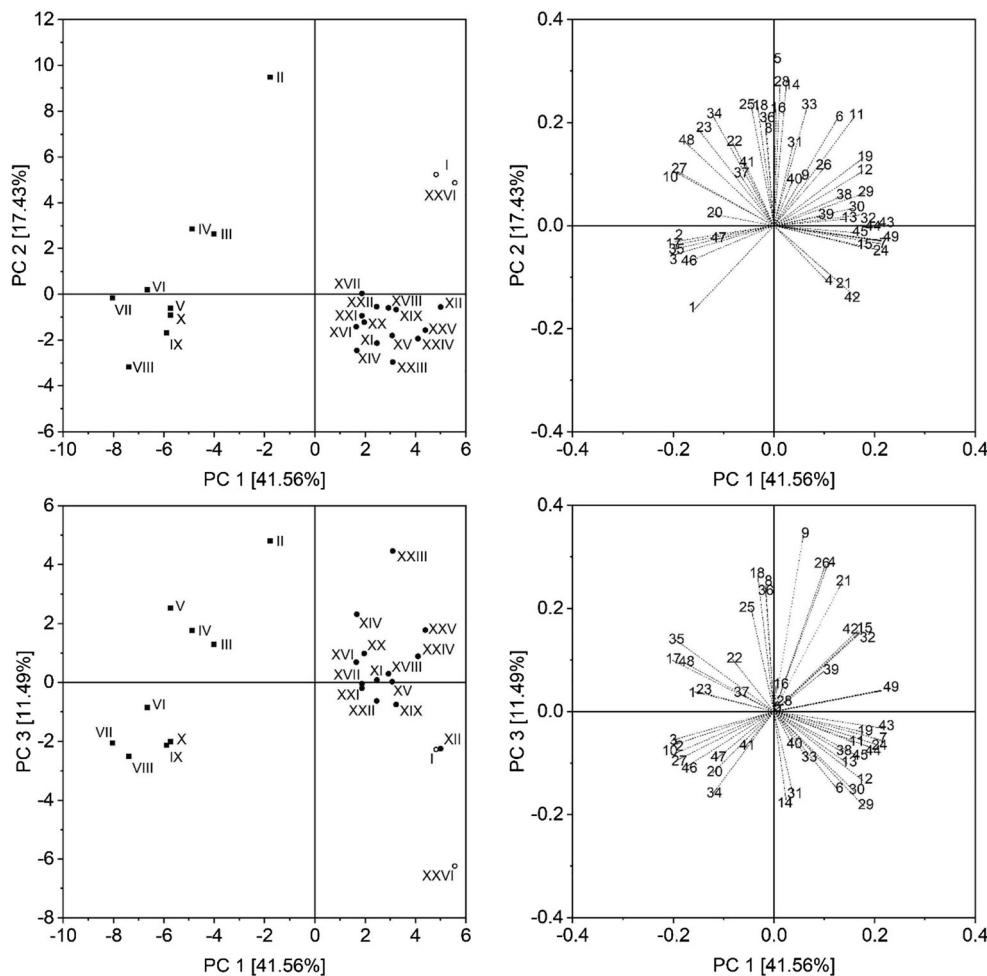


Fig. 1 Contributions of the variables to the PCs within PCA-1. The dashed line indicates the cut-off value represented as average contribution of 2.0%

Fig. 2 Score plots (left) and loading plots (right) for PCA-1 (non-filled circles: wood pellets; filled circles: wood chips; filled squares: Miscanthus and straw pellets as well as blended biomass pellets)



contamination. Finally, PC3 described 11.49% of the total data variance and highlighted dissimilarities with regard to possible contaminations between the fuel blends with *Miscanthus* and wood (object II to V), soil contaminated wood chip batch 2-R (object XXIII) and woody biomass (object I, XII, and especially XXVI). Contents of Al and Fe both in the fuel and bottom ash (variables 4, 9, 21, and 26) were the variables with the highest contribution for wood chips (i.e., 6-R, object XXIII). For *Miscanthus* and blends with wood (objects II to V), Cr and Ti both in the fuel and bottom ash were the most important contributors (variables 8, 18, 25, and 36).

For PCA-2, the first three PCs describe 80.52% of the total data variance and for five PCs eigenvalues exceeding than one have been calculated (Table S13). Analogous to PCA-1, only three PCs were considered for further evaluation as PC4 described only 5.76% and PC5 only 3.57% of the total data variance.

In Fig. 3, contributions of the variables to the three PCs within PCA-2 are displayed. The cut-off value calculated as the average contribution was 3.6%. Calculation of the cut-off value according to uniform contribution of the 29 variables resulted also in 3.6%. Accordingly, parameters describing bottom ash slagging during biomass combustion such as K in the fuel, DT, HT, characteristic slagging categories (i.e., BAFS > 63 mm, BAFS 16–45 mm, and BAFS < 16 mm) as well as DT-HT range, molar ratio $Si/(Ca + Mg)$, and $(Si + P + K)/(Ca + Mg)$ are contributing to PC1 (variables 43, 44, 46, 48, 49, 50, 52, 53, and 69). Both coal indices S_R and SA are also contributing to PC1 (variables 59 and 65). Interestingly, a rather uniform contribution of all these variables to PC1 was observed. Indices such as B/A, B/A + P, Rs, Fu, Cl, and S ratio (variables 60, 61, 63, 64, 66, and 67) are contributing mostly to PC2. PC3 is mainly described by indices relevant for fuel contamination such as Si/K, Al/200, Fe/Mn, and DAI (variables 50, 56, 57, and 58). Also, BAI index (variable 62) is contributing significantly to PC3. The parameters SST, FT, BAFS 45–63 mm, and the molar ratio of $(K + Na)/(2S + Cl)$ and Si/K (variables 42, 45, 46, 51, and 55) did not considerably contribute to PC1, PC2, and PC3 within PCA-2.

Score and loading plots for PCA-2 are presented in Fig. 4. As for PCA-1, two groups, i.e., woody biomass fuels (objects I and XI to XXVI) and blended biomass fuels (objects II to X), can be distinguished. According to PC1, describing 46.01% of the total data variance, the investigated fuels can be distinguished according to indices for bottom ash slagging which were initially developed for biomass combustion. For woody biomass, the largest contribution originates from DT, HT, and negligible slagging indicated by BAFS < 16 mm (variables 43, 44, and 49). In contrast, positions of fuel blends with wheat straw (objects V to X) in the score plot are mainly influenced by the variable K content in the fuel, $Si/(Ca + Mg)$, $(Si + P + K)/(Ca + Mg)$, SA and S_R (variables 50, 52, 53, 59, and 65). PC2 accounted for 27.02% of the total data

variance. Interestingly, in PCA-2, blended and herbaceous fuels (object II to X) scattered much less along PC2 than in PCA-1. Also for woody biomass, PC2 does not show much variation except for the pure wood pellets (object I and XXVI) and for 2-R and 6-R (object XIII and XXIII). Accordingly, it seems that the slagging indices B/A, B/A + P, SST-DT range, Rs, Fu, Cl, and S ratio (variables 60, 61, 63, 64, 66, 67, and 68) might not be suitable to differentiate between the investigated biomass fuels. Only for clean wood pellets (object I and XXVI), these variables resulted in a large variance, which is probably due to their low Si and Al content relative to the Ca content in the fuel. PC3 described 7.49% of the total data variance allowing for the differentiation of the investigated fuels with respect to indices describing fuel contamination. Only reference fuel XXVI (wood pellets) and the fuels 100M, 2-R, and 6-R (objects V, XIII, and XXIII) were substantially different to their PC3 values. This can be rationalized by the highest Al/200 values (variable 56) which were calculated for wood chip batches 2-R and 6-R (object XIII and XXIII) as well as particularly high values for Si/K and Fe/Mn (variable 54 and 57). For fuel 100M (object V), Al/200, molar Si/K ratio, and DAI (variables 54, 56, and 58) are highest among all blended and herbaceous fuels. In contrast, position of reference fuel XXVI (wood pellets) in the score plot for PC3 in Fig. 4 may result from particularly high indices $(K + Na)/(2S + Cl)$, B/A, B/A + P, Fu, S_R , Cl, and S ratio, though their contribution to PC3 is rather low (Table 5).

Concisely, PCA results underscore that the molar index $(Si + P + K)/(Ca + Mg)$, i.e., variable 53, mostly provides a good indication for the estimation of bottom ash slagging. However, S and Cl also seem to have a certain relevance in this context. These elements as well as Al as strong indicator for soil contamination should also be considered for the further development of the slagging index.

3.2 Description of bottom ash slagging

The most commonly used parameters to estimate the potential slagging risk in the bottom ash are the characteristic ash melting temperatures SST, DT, HT, and FT determined for the fuel ash following standardized procedures [83]. If DT and HT are well above boiler temperatures, slagging risk is considered low. However, real slag formation at certain combustion temperatures is poorly described by this method and ash melting may result in different structures of the slag being more or less critical for boiler operation. This problem was addressed by defining different sinter categories and determination of slag fractions by means of sieving [23, 44]. The amount of ash that potentially forms slags is important in any case. Inspired by the work of Schwabl et al. [71] and as a result of the relevance of ash content (variable 1) as well as bottom ash fraction that forms slag (BAFS, variable 46

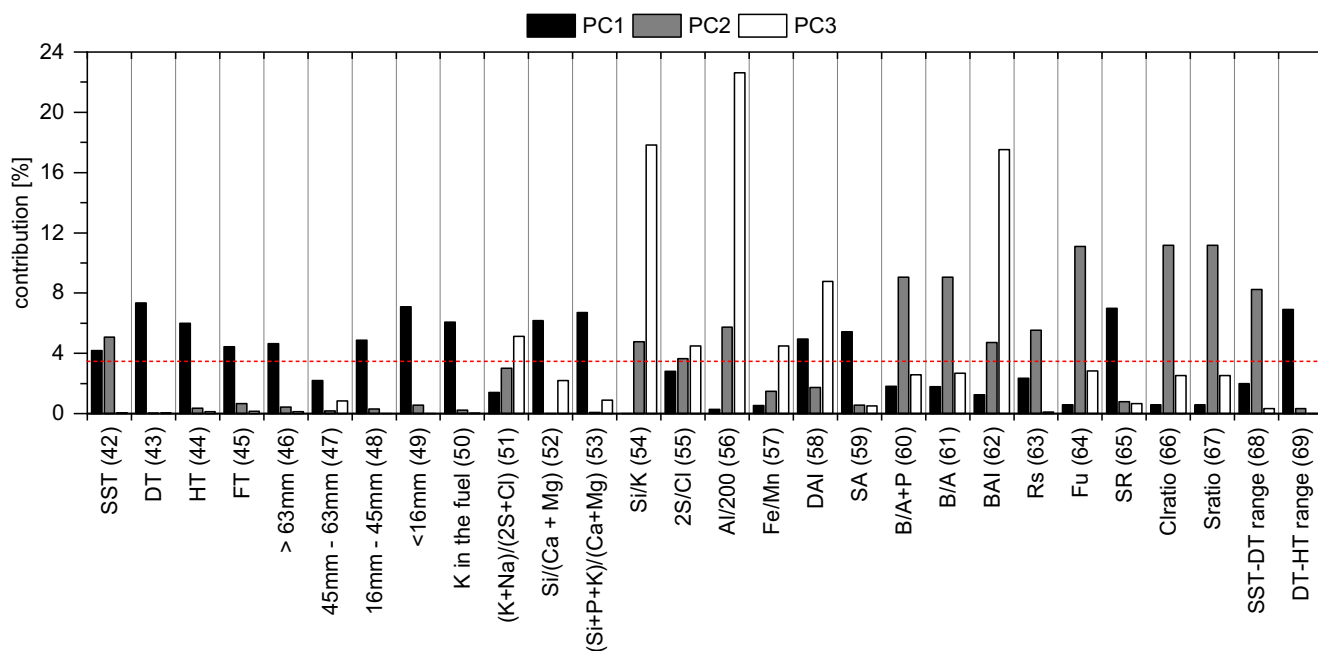
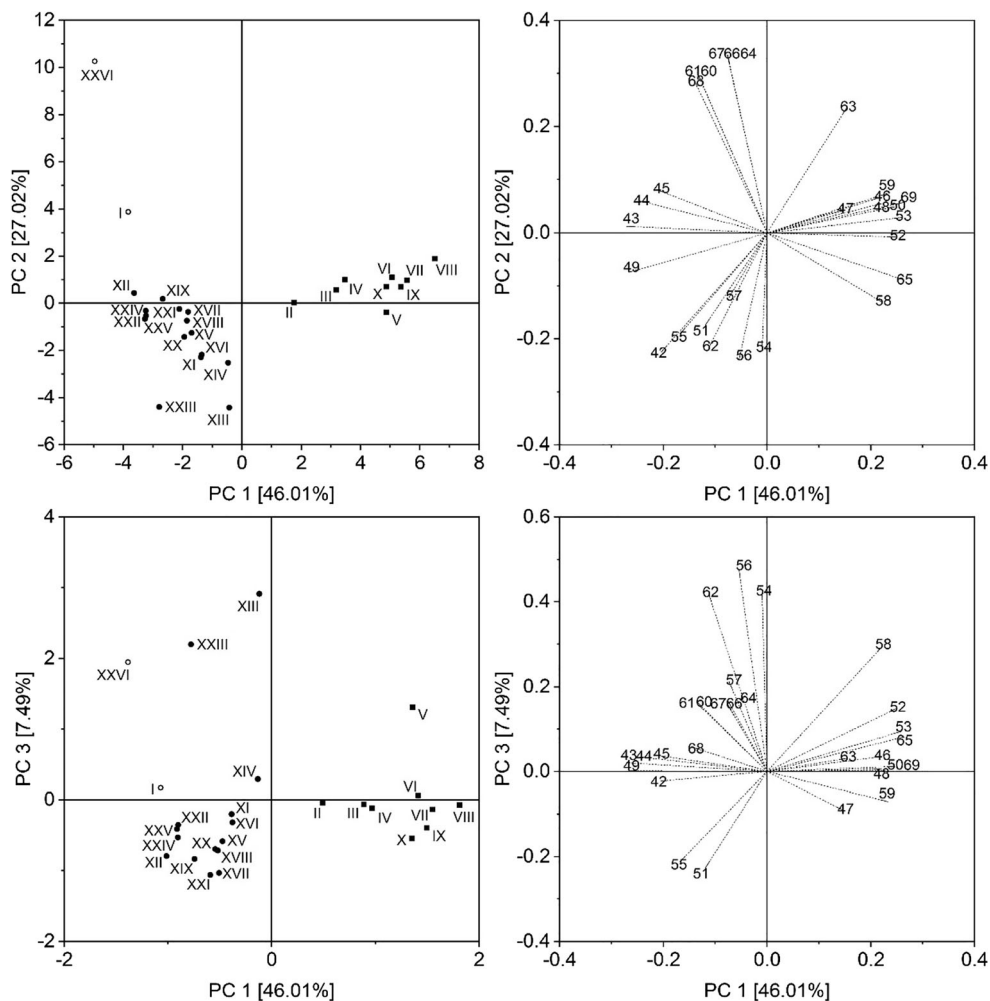


Fig. 3 Contributions of the variables to the PCs within PCA-2. The dashed line indicates the cut-off value represented as average contribution of 3.6%

Fig. 4 Score plots (left) and loading plots (right) for PCA-2 (non-filled circles: wood pellets; filled circles: wood chips; filled squares: Miscanthus and straw pellets as well as blended biomass pellets)



and 49) for PC-1 in PCA-1, the new parameter susceptibility to slag formation (SSF) was developed which is defined using the normalized ash content ($A_N = A_i/A_{\max}$), normalized bottom ash fraction that forms slag > 16 mm ($SF_N = SF_i/SF_{\max}$), and the normalized sinter category ($S_N = S_i/S_{\max}$) among the investigated fuels and by implementing the arithmetic mean of the three parameters (i.e., each parameter has the same importance for the SSF) (Eq. 2).

$$SSF = \frac{A_N + SF_N + S_N}{3} [-] \quad (2)$$

3.3 Adaption of the slagging index

The ash transformation behavior is yet not fully understood especially at low oxygen atmospheres (i.e., during pyrolysis and gasification) influencing the decomposition of the organic and inorganic fractions, and consequently the release patterns especially of K, S, and Cl at a given conversion temperature [84–92]. Especially, K and its association with other ash components plays a prominent role during melt formation in the bottom ash. During combustion, K release is facilitated by the presence of Cl as KCl or for hydrous systems as KOH. Potassium, which is retained in the bottom ash, can be incorporated in silicate melts or minerals as well as salt melts (with Cl) and sulfates [14, 85–87, 93].

Attempts to estimate bottom ash slagging in small-scale appliances with fuel indices provided in several cases contradictory results [15, 18, 21, 43]. Thermodynamic equilibrium (TEC) calculations are often considered a promising alternative for the prediction of bottom ash slagging [34, 94]. However, reliable results are strongly depending on the quality as well as the selection and individual modification of the thermodynamic databases and assumption of a realistic oxygen atmosphere in the fuel bed, which can have tremendous impact on the obtained results. A further drawback in interpreting TEC results is the limitation to fully stable phases (i.e., with an activity of one) and equilibrium conditions that cannot be guaranteed in all cases. In order to make these calculations applicable in a general way, a careful and comprehensive validation is still needed. Therefore, despite its well-reported shortcomings, fuel indices still can provide a simple and straightforward method to estimate bottom ash slagging and should be further developed for specific applications.

Based on the obtained PCA-1 results for wood chips and pellets, herbaceous biomass (wheat straw and Miscanthus), and biomass fuel blends, it was shown that Si, Ca, K, and Mg in the bottom ash (variables 24, 27, 29, and 35) are relevant components in the context of bottom ash slagging. The molar ratio $(Si + P + K)/(Ca + Mg)$, i.e.,

variable 53, seems to be the most suitable fuel index to estimate bottom ash slagging as also highlighted by PCA-2. Though correlation of the molar ratio $(Si + P + K)/(Ca + Mg)$ with the proposed SSF parameter (Eq. 2) provides a quite satisfying determination coefficient of 0.83 (Fig. 5, left), the position of some fuels—in particular fuel V (100M) and VIII (100S)—does not reflect the observed bottom ash slagging behavior. The most critical slagging behavior was observed for 100S (fuel VIII) followed by 100M (fuel V) which is well represented by their SSF values 1.0 and 0.83, respectively. However, according to the molar ratio $(Si + P + K)/(Ca + Mg)$, a less severe slagging would be expected.

To improve the applicability of this fuel index, further elements may be incorporated. Al can be introduced in the fuel by sand, soil, or clay (e.g., in the form of feldspars or clay minerals) [17] which can be accompanied by Si resulting in different Si/Al ratios. However, compared to Si, Al is more effective in increasing ash melting temperatures [95]. Depending on the origin of Al (i.e., as kaolinite (Al-silicate), K-feldspar, Ca-feldspar, etc.), differences in the reactivity of Al during ash transformation reactions and their ability to capture alkali compounds and influence melt formation might be possible [28, 96–99]. Sommersacher et al. already suggested to include Al in the molar ratio $(Si + P + K)/(Ca + Mg)$ for those fuels containing Al-rich additives such as kaolin [37]. Therefore, the incorporation of Al might also be appropriate for the estimation of bottom ash slagging if fuel contamination is expected, Eq. 3. This is also supported by PCA-1.

$$\text{slag index}_{Al} = \frac{Si + P + K}{Ca + Mg + Al} [\text{mol/mol}] \quad (3)$$

The correlation of the molar ratio $(Si + P + K)/(Ca + Mg + Al)$ with the proposed SSF parameter provides a slightly improved determination coefficient of 0.86. However, likewise to Fig. 5 (left), the position of some fuels does still not reflect the observed bottom ash slagging behavior. As shown by PCA-1, Cl and S might also be relevant for the estimation of bottom ash slagging. Though Cl was found in some cases in bottom ashes obtained from the combustion of Cl-rich biomasses [93, 100–102], most studies show that it is usually almost completely released to the gas phase [14, 103–105]. In contrast, a high share of K_2SO_4 was found in the slag and non-slag fraction of bottom ashes especially from the combustion of Miscanthus and wheat straw which might additionally be facilitated if conversion temperatures are below 1000 °C [101, 102, 106–108]. With the Babcock Index (Table 2), an estimation of slag formation in different ash fractions was suggested for the

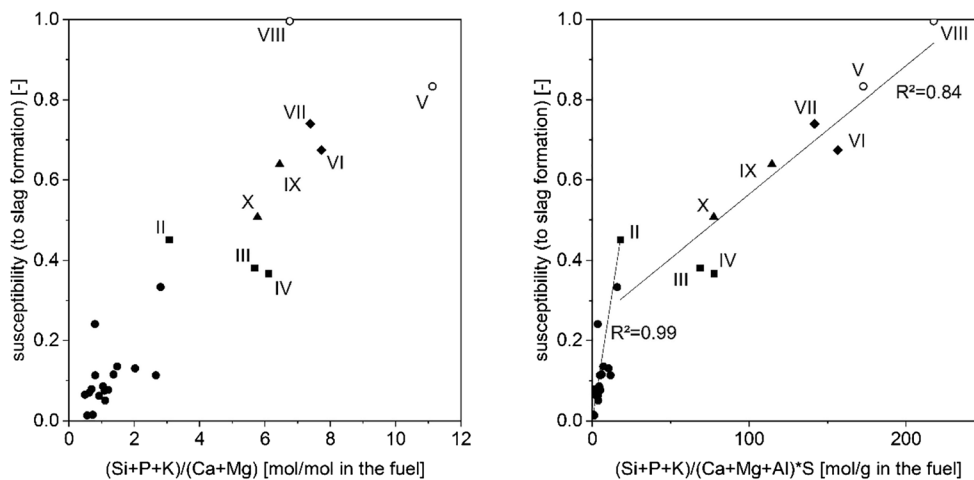


Fig. 5 Molar ratio of (Si + P + K)/(Ca + Mg), left, and (Si + P + K)/(Ca + Mg + Al) × S, right, versus SSF. Black filled circles: wood pellets and wood chips (objects I and XI to XXVI); black filled squares: W/M pellet blends (objects II to IV); black filled triangles: W/S pellet blends (object

IX and X); black filled diamond: M/S pellet blends (object VI and VII); non filled circles: herbaceous biomass pellets, i.e., 100M and 100S (object V and VIII)

combustion of bituminous and brown coal [19]. Likewise, the molar ratio (Si + P + K)/(Ca + Mg) should be adapted by S, Eq. 4.

$$\text{slag index}_{\text{Al,S}} = \left(\frac{\text{Si} + \text{P} + \text{K}}{\text{Ca} + \text{Mg} + \text{Al}} \right) \cdot \text{S} \text{ [mol/g]} \quad (4)$$

Applying the adapted slag index (Eq. 4) to the SSF, it becomes apparent that this index can be a useful estimation tool for bottom ash slagging (Fig. 5) (right).

Compared to Fig. 5 (left), a clear separation between woody and blended as well as herbaceous biomass fuels becomes apparent. For woody biomass fuels, the determination coefficient is 0.99, while for blended and herbaceous biomass fuels, a determination coefficient of 0.84 is achieved. Three ranges can be distinguished for (Si + P + K)/(Ca + Mg + Al) × S:

- A. (Si + P + K)/(Ca + Mg + Al) × S < 20 mol/g: low susceptibility to slag formation (i.e., SSF < 0.4, including wood pellets and wood chips, objects I and XI to XXVI, not labeled in Fig. 5). Fuels in this range are characterized by an ash content of up to 7 wt% d.b., BAFS > 16 mm below 5% and a sinter category of 1.
- B. (Si + P + K)/(Ca + Mg + Al) × S = 20–75 mol/g: elevated susceptibility to slag formation (i.e., SSF = 0.4–0.6, including W/M pellet blends (objects II–IV) and 70W30S pellet blend (object X). Fuels in this range are characterized by an ash content of up to 3 wt% d.b., BAFS > 16 mm between 30 and 50% and a sinter category between 2 and 3.
- C. (Si + P + K)/(Ca + Mg + Al) × S > 75 mol/g: serious susceptibility to slag formation (i.e., SSF > 0.6), including 100M, 100S, M/S pellet blends, and 30W70S pellet blend

(objects V–IX). Fuels in this range are characterized by an ash content between 4 and 7 wt% d.b., BAFS > 16 mm between 40 and 60%, and a sinter category between 3 and 4.

The transition between ranges A and B can be marked by object II (which was considered in both correlations in Fig. 5). It was shown by Zeng et al. that this fuel blend (i.e., 70 wt% wood sawdust and 30 wt% Miscanthus) was characterized by an ash behavior which displays the transition between wood and straw-like fuels [39]. Accordingly, with the adapted slag index, the differences in the slagging behavior in the bottom ash during the combustion of woody and herbaceous biomass fuels can be well distinguished and estimated.

4 Summary and conclusions

In this work, experimental data derived from two combustion test campaigns with an automatically stoked small-scale boiler were investigated by principal component analysis. Based on this, the complex interdependencies between the fuel composition and the resulting bottom ash characteristics and the applicability of existing fuel indices were evaluated. The principal component analysis highlighted that Si, Ca, K, and Mg and also the remaining Al and S in the bottom ash are crucial fuel components in the context of bottom ash melting. Thus, the molar ratio (Si + P + K)/(Ca + Mg) was adapted by Al and S and correlated with the susceptibility to slag formation based on the arithmetic mean of the normalized ash content,

normalized bottom ash fraction that forms slag > 16 mm as well as the normalized sinter category among the investigated fuels. Thus, the applicability of the slag index was evaluated with respect to the bottom ash slagging risk during real-scale combustion. Three ranges were distinguished for the fuel index corresponding to a specific susceptibility to slag formation (i.e., low < 20 mol/g for woody biomass as well as elevated between 20 and 75 mol/g and serious > 75 mol/g for straw-like fuels and blends with wood). The linear regression of the slag index with susceptibility to slag formation exhibits a high coefficient of determination (i.e., 0.99 for woody biomass and 0.84 for straw-like fuels and blends with wood). This fuel index can be applied for grate combustion in automatically stoked small-scale boilers fueled with woody biomass, Miscanthus, and wheat straw as well as blends thereof. In future investigations, the fuel index may prove to be suitable for further combustion technologies (and therefore dedicated oxygen atmospheres during the conversion steps) and other fuel assortments such as agricultural biomass with critical composition, demolition wood, or sewage sludge. The suggested susceptibility to slag formation (SSF) parameter might prove to be a more suitable parameter for the evaluation of slagging risk in real-scale boiler operation.

Funding The data sets used in this publication were funded under grant agreement number 22031814, 22035714, 22035814, and 22005815 of the Agency for Renewable Resources (Fachagentur Nachwachsende Rohstoffe e.V., FNR) in the name of the German Federal Ministry of Food and Agriculture (BMEL) on the basis of a resolution of the German Federal Parliament and upon work supported by the German Federal Ministry of Education and Research (BMBF) under Grant No. 03SF0347B. A.M.M. was supported by DAAD for an internship in DBFZ Deutsches Biomasseforschungszentrum gemeinnützige GmbH (DBFZ) through Research Grants - Short-Term Grants 2018 Program (funding program no. 57378443). Furthermore, funds of the Federal Ministry of Food and Agriculture (BMEL) supported this work based on a decision of the Parliament of the Federal Republic of Germany via the Federal Office for Agriculture and Food (BLE) under the innovation support program.

References

- United Nations Framework Convention on Climate Change (2015) Adoption of the Paris Agreement: Proposal by the President. Paris Climate Change Conference - November 2015, Cop 21, Paris, France
- Bundesministerium für Umwelt, Naturschutz und Reaktorsicherheit (2016) Klimaschutzplan 2050: Klimaschutzpolitische Grundsätze und Ziele der Bundesregierung, Berlin, Germany
- Intergovernmental Panel on Climate Change (2018) Global warming of 1.5°C. An IPCC Special Report on the impacts of global warming of 1.5°C above pre-industrial levels and related global greenhouse gas emission pathways, in the context of strengthening the global response to the threat of climate change, sustainable development, and efforts to eradicate poverty: Summary for Policymakers
- Steffen W, Rockström J, Richardson K, Lenton TM, Folke C, Liverman D, Summerhayes CP, Barnosky AD, Cornell SE, Crucifix M, Donges JF, Fetzer I, Lade SJ, Scheffer M, Winkelmann R, Schellnhuber HJ (2018) Trajectories of the earth system in the Anthropocene. *Proc Natl Acad Sci* 115:8252–8259. <https://doi.org/10.1073/pnas.1810141115>
- Smith CJ, Forster PM, Allen M, Fuglestedt J, Millar RJ, Rogelj J, Zickfeld K (2019) Current fossil fuel infrastructure does not yet commit us to 1.5 °C warming. *Nat Commun* 10(1):101. <https://doi.org/10.1038/s41467-018-07999-w>
- (2018) AGEBA - Zusammenfassung Anwendungsbilanzen für die Endenergiesektoren 2013 bis 2016, Berlin, Germany
- Szarka N, Scholwin F, Trommler M, Fabian Jacobi H, Eichhorn M, Ortwein A, Thrän D (2013) A novel role for bioenergy: a flexible, demand-oriented power supply. *Energy* 61:18–26. <https://doi.org/10.1016/j.energy.2012.12.053>
- Thrän D (2015) Smart bioenergy: technologies and concepts for a more flexible bioenergy provision in future energy systems. Springer International Publishing
- Brosowski A, Thrän D, Mantau U, Mahro B, Erdmann G, Adler P, Stinner W, Reinhold G, Hering T, Blanke C (2016) A review of biomass potential and current utilisation – status quo for 93 biogenic wastes and residues in Germany. *Biomass Bioenergy* 95: 257–272. <https://doi.org/10.1016/j.biombioe.2016.10.017>
- Vassilev SV, Baxter D, Andersen LK, Vassileva CG (2010) An overview of the chemical composition of biomass. *Fuel* 89(5): 913–933. <https://doi.org/10.1016/j.fuel.2009.10.022>
- Boström D, Skoglund N, Grimm A, Boman C, Öhman M, Broström M, Backman R (2012) Ash transformation chemistry during combustion of biomass. *Energy Fuel* 26(1):85–93. <https://doi.org/10.1021/ef201205b>
- Dietz E, Kuptz D, Blum U, Schulmeyer F, Borchert H, Hartmann H (2016) New indexes for the contamination of wood chips with mineral soil. In: ETA-Florence renewable energies (ed) proceedings of the 24th European biomass conference and exhibition, Florence, pp 630–633
- Vassilev SV, Vassileva CG, Song Y-C, Li WY, Feng J (2017) Ash contents and ash-forming elements of biomass and their significance for solid biofuel combustion. *Fuel* 208:377–409. <https://doi.org/10.1016/j.fuel.2017.07.036>
- Knudsen JN, Jensen PA, Dam-Johansen K (2004) Transformation and release to the gas phase of Cl, K, and S during combustion of annual biomass. *Energy Fuel* 18(5):1385–1399. <https://doi.org/10.1021/ef049944q>
- Sommersacher P, Brunner T, Oberberger I (2012) Fuel indexes: a novel method for the evaluation of relevant combustion properties of new biomass fuels. *Energy Fuel* 26(1):380–390. <https://doi.org/10.1021/ef201282y>
- Vassilev SV, Baxter D, Vassileva CG (2014) An overview of the behaviour of biomass during combustion: part II. Ash fusion and ash formation mechanisms of biomass types. *Fuel* 117:152–183. <https://doi.org/10.1016/j.fuel.2013.09.024>
- Vassilev SV, Baxter D, Andersen LK, Vassileva CG, Morgan TJ (2012) An overview of the organic and inorganic phase composition of biomass. *Fuel* 94:1–33. <https://doi.org/10.1016/j.fuel.2011.09.030>
- Gilbe C, Lindström E, Backman R, Samuelsson R, Burvall J, Ohman M (2008) Predicting slagging tendencies for biomass pellets fired in residential appliances: a comparison of different prediction methods. *Energy Fuel* 22(6):3680–3686. <https://doi.org/10.1021/ef800321h>
- Pronobis M (2005) Evaluation of the influence of biomass combustion on boiler furnace slagging by means of fusibility correlations. *Biomass Bioenergy* 28(4):375–383. <https://doi.org/10.1016/j.biombioe.2004.11.003>

20. Vamvuka D, Zografos D (2004) Predicting the behaviour of ash from agricultural wastes during combustion. *Fuel* 83(14–15): 2051–2057. <https://doi.org/10.1016/j.fuel.2004.04.012>
21. Lindström E, Öhman M, Backman R, Boström D (2008) Influence of sand contamination on slag formation during combustion of wood derived fuels. *Energy Fuel* 22(4):2216–2220. <https://doi.org/10.1021/ef700772q>
22. Díaz-Ramírez M, Boman C, Sebastián F, Royo J, Xiong S, Boström D (2012) Ash characterization and transformation behavior of the fixed-bed combustion of novel crops: poplar, brassica, and cassava fuels. *Energy Fuel* 26(6):3218–3229. <https://doi.org/10.1021/ef2018622>
23. Öhman M, Boman C, Hedman H, Nordin A, Boström D (2004) Slagging tendencies of wood pellet ash during combustion in residential pellet burners. *Biomass Bioenergy* 27(6):585–596. <https://doi.org/10.1016/j.biombioe.2003.08.016>
24. Bryers RW (1996) Fireside slagging, fouling, and high-temperature corrosion of heat-transfer surface due to impurities in steam-raising fuels. *Prog Energy Combust Sci* 22(1):29–120. [https://doi.org/10.1016/0360-1285\(95\)00012-7](https://doi.org/10.1016/0360-1285(95)00012-7)
25. Jenkins BM, Baxter LL, Miles TR (1998) Combustion properties of biomass. *Fuel Process Technol* 54(1–3):17–46. [https://doi.org/10.1016/S0378-3820\(97\)00059-3](https://doi.org/10.1016/S0378-3820(97)00059-3)
26. Garcia-Maraver A, Mata-Sanchez J, Carpio M, Perez-Jimenez JA (2017) Critical review of predictive coefficients for biomass ash deposition tendency. *J Energy Inst* 90(2):214–228. <https://doi.org/10.1016/j.joei.2016.02.002>
27. Basu P, Kefa C, Jestin L (2000) Corrosion and fouling of heat transfer surfaces. In: Basu P, Kefa C, Jestin L (eds) *Boilers and burners: design and theory*. Springer New York, New York, NY, pp 385–425
28. Niu Y, Zhu Y, Tan H, Hui S, Jing Z, Xu W (2014) Investigations on biomass slagging in utility boiler: criterion numbers and slagging growth mechanisms. *Fuel Process Technol* 128:499–508. <https://doi.org/10.1016/j.fuproc.2014.07.038>
29. Vamvuka D, Zografos D, Alevizos G (2008) Control methods for mitigating biomass ash-related problems in fluidized beds. *Bioresour Technol* 99(9):3534–3544. <https://doi.org/10.1016/j.biortech.2007.07.049>
30. Pronobis M, Kalisz S, Polok M (2013) The impact of coal characteristics on the fouling of stoker-fired boiler convection surfaces. *Fuel* 112:473–482. <https://doi.org/10.1016/j.fuel.2013.05.044>
31. Lindström E, Sandström M, Boström D, Öhman M (2007) Slagging characteristics during combustion of cereal grains rich in phosphorus. *Energy Fuel* 21(2):710–717. <https://doi.org/10.1021/ef060429x>
32. Sommersacher P, Brunner T, Oberberger I, Kienzl N, Kanzian W (2015) Combustion related characterisation of Miscanthus peat blends applying novel fuel characterisation tools. *Fuel* 158:253–262. <https://doi.org/10.1016/j.fuel.2015.05.037>
33. Wiinikka H, Gebart R, Boman C, Boström D, Öhman M (2007) Influence of fuel ash composition on high temperature aerosol formation in fixed bed combustion of woody biomass pellets. *Fuel* 86(1–2):181–193. <https://doi.org/10.1016/j.fuel.2006.07.001>
34. Lindberg D, Backman R, Chartrand P, Hupa M (2013) Towards a comprehensive thermodynamic database for ash-forming elements in biomass and waste combustion — current situation and future developments. *Fuel Process Technol* 105:129–141. <https://doi.org/10.1016/j.fuproc.2011.08.008>
35. Rizvi T, Xing P, Pourkashanian M, Darvell LI, Jones JM, Nimmo W (2015) Prediction of biomass ash fusion behaviour by the use of detailed characterisation methods coupled with thermodynamic analysis. *Fuel* 141:275–284. <https://doi.org/10.1016/j.fuel.2014.10.021>
36. Paulrud S, Nilsson C, Öhman M (2001) Reed canary-grass ash composition and its melting behaviour during combustion. *Fuel* 80(10):1391–1398. [https://doi.org/10.1016/S0016-2361\(01\)00003-5](https://doi.org/10.1016/S0016-2361(01)00003-5)
37. Sommersacher P, Brunner T, Oberberger I, Kienzl N, Kanzian W (2013) Application of novel and advanced fuel characterization tools for the combustion related characterization of different wood/kaolin and straw/kaolin mixtures. *Energy Fuel* 27(9): 5192–5206. <https://doi.org/10.1021/ef400400n>
38. Zeng T, Pollex A, Weller N, Lenz V, Nelles M (2018) Blended biomass pellets as fuel for small scale combustion appliances: effect of blending on slag formation in the bottom ash and pre-evaluation options. *Fuel* 212:108–116. <https://doi.org/10.1016/j.fuel.2017.10.036>
39. Zeng T, Weller N, Pollex A, Lenz V (2016) Blended biomass pellets as fuel for small scale combustion appliances: influence on gaseous and total particulate matter emissions and applicability of fuel indices. *Fuel* 184:689–700. <https://doi.org/10.1016/j.fuel.2016.07.047>
40. Kuptz D, Schreiber K, Schulmeyer F, Lesche S, Zeng T, Ahrens F, Zelinski V, Schön C, Pollex A, Borchert H, Lenz V, Loewen A, Nelles M, Hartmann H (2019) Evaluation of combined screening and drying steps for the improvement of the fuel quality of forest residue wood chips - results from six case studies. *Biomass Conv Bioref* 81(3):356. <https://doi.org/10.1007/s13399-019-00389-2>
41. Schön C, Kuptz D, Mack R, Zelinski V, Loewen A, Hartmann H (2019) Influence of wood chip quality on emission behaviour in small-scale wood chip boilers. *Biomass Conv Bioref* 9(1):71–82. <https://doi.org/10.1007/s13399-017-0249-7>
42. Zeng T, Kuptz D, Schreiber K, Schön C, Schulmeyer F, Zelinski V, Pollex A, Borchert H, Loewen A, Hartmann H, Lenz V, Nelles M (2019) Impact of adhering soil and other extraneous impurities on the combustion and emission behavior of forest residue wood chips in an automatically stoked small-scale boiler. *Biomass Conv Bioref* 5(1):35. <https://doi.org/10.1007/s13399-018-00368-z>
43. Näzelius I-L, Boström D, Rebbing A, Boman C, Öhman M (2017) Fuel indices for estimation of slagging of phosphorus-poor biomass in fixed bed combustion. *Energy Fuel* 31(1):904–915. <https://doi.org/10.1021/acs.energyfuels.6b02563>
44. Fernández MJ, Mediavilla I, Barro R, Borjabad E, Ramos R, Carrasco JE (2019) Sintering reduction of herbaceous biomass when blended with woody biomass: predictive and combustion tests. *Fuel* 239:1115–1124. <https://doi.org/10.1016/j.fuel.2018.11.115>
45. Škrbić BD, Cvejanov J, Đurišić-Mladenović N (2015) Chemometric characterization of vegetable oils based on the fatty acid profiles for selection of potential feedstocks for biodiesel production. *J. Biobased Mater. Bioenergy* 9(3):358–371. <https://doi.org/10.1166/jbmb.2015.1527>
46. Eide I, Zahlens K (2007) Chemical fingerprinting of biodiesel using electrospray mass spectrometry and chemometrics: characterization, discrimination, identification, and quantification in petrodiesel. *Energy Fuel* 21(6):3702–3708. <https://doi.org/10.1021/ef700342f>
47. Flood ME, Goding JC, O'Connor JB, Ragon DY, Hupp AM (2014) Analysis of biodiesel feedstock using GCMS and unsupervised chemometric methods. *J Am Oil Chem Soc* 91(8):1443–1452. <https://doi.org/10.1007/s11746-014-2488-0>
48. Hupp AM, Marshall LJ, Campbell DI, Smith RW, McGuffin VL (2008) Chemometric analysis of diesel fuel for forensic and environmental applications. *Anal Chim Acta* 606(2):159–171. <https://doi.org/10.1016/j.aca.2007.11.007>
49. Kim K, Labbé N, Warren JM, Elder T, Rials TG (2015) Chemical and anatomical changes in Liquidambar styraciflua L. xylem after long term exposure to elevated CO₂. *Environ Pollut* 198:179–185. <https://doi.org/10.1016/j.envpol.2015.01.006>
50. Toscano G, Rinnan Å, Pizzi A, Mancini M (2017) The use of near-infrared (NIR) spectroscopy and principal component analysis

- (PCA) to discriminate bark and wood of the most common species of the pellet sector. *Energy Fuel* 31(3):2814–2821. <https://doi.org/10.1021/acs.energyfuels.6b02421>
51. Mancini M, Rinnan Å, Pizzi A, Mengarelli C, Rossini G, Duca D, Toscano G (2018) Near infrared spectroscopy for the discrimination between different residues of the wood processing industry in the pellet sector. *Fuel* 217:650–655. <https://doi.org/10.1016/j.fuel.2018.01.008>
 52. Friedl A, Padouvas E, Rotter H, Varmuza K (2005) Prediction of heating values of biomass fuel from elemental composition. *Anal Chim Acta* 544(1):191–198. <https://doi.org/10.1016/j.aca.2005.01.041>
 53. Pommer L, Öhman M, Boström D, Burvall J, Backman R, Olofsson I, Nordin A (2009) Mechanisms behind the positive effects on bed agglomeration and deposit formation combusting forest residue with peat additives in fluidized beds. *Energy Fuel* 23(9):4245–4253. <https://doi.org/10.1021/ef900146e>
 54. Tao G, Geladi P, Lestander TA, Xiong S (2012) Biomass properties in association with plant species and assortments. II: a synthesis based on literature data for ash elements. *Renew Sust Energy Rev* 16(5):3507–3522. <https://doi.org/10.1016/j.rser.2012.01.023>
 55. Tao G, Lestander TA, Geladi P, Xiong S (2012) Biomass properties in association with plant species and assortments I: a synthesis based on literature data of energy properties. *Renew Sust Energy Rev* 16(5):3481–3506. <https://doi.org/10.1016/j.rser.2012.02.039>
 56. Sad CMS, da Silva M, dos Santos FD, Pereira LB, Corona RRB, Silva SRC, Portela NA, Castro EVR, Filgueiras PR, Lacerda V Jr (2019) Multivariate data analysis applied in the evaluation of crude oil blends. *Fuel* 239:421–428. <https://doi.org/10.1016/j.fuel.2018.11.045>
 57. Voshell S, Mäkelä M, Dahl O (2018) A review of biomass ash properties towards treatment and recycling. *Renew Sust Energy Rev* 96:479–486. <https://doi.org/10.1016/j.rser.2018.07.025>
 58. Dellavedova M, Derudi M, Biesuz R, Lunghi A, Rota R (2012) On the gasification of biomass: data analysis and regressions. *Process Saf Environ Prot* 90(3):246–254. <https://doi.org/10.1016/j.psep.2011.08.001>
 59. Đurišić-Mladenović N, Škrbić BD, Zabaniotou A (2016) Chemometric interpretation of different biomass gasification processes based on the syngas quality: assessment of crude glycerol co-gasification with lignocellulosic biomass. *Renew Sust Energy Rev* 59:649–661. <https://doi.org/10.1016/j.rser.2016.01.002>
 60. Škrbić BD, Đurišić-Mladenović N, Cvejanov J (2018) Differentiation of syngases produced by steam gasification of mono- and mixed sources feedstock: a chemometric approach. *Energy Convers Manag* 171:1193–1201. <https://doi.org/10.1016/j.enconman.2018.06.060>
 61. Manyà JJ, Ruiz J, Arauzo J (2007) Some peculiarities of conventional pyrolysis of several agricultural residues in a packed bed reactor. *Ind Eng Chem Res* 46(26):9061–9070. <https://doi.org/10.1021/ie070811c>
 62. Pattiya A, Titiloye JO, Bridgwater AV (2010) Evaluation of catalytic pyrolysis of cassava rhizome by principal component analysis. *Fuel* 89(1):244–253. <https://doi.org/10.1016/j.fuel.2009.07.003>
 63. Acquah GE, Via BK, Fasina OO, Adhikari S, Billor N, Eckhardt LG (2017) Chemometric modeling of thermogravimetric data for the compositional analysis of forest biomass. *PLoS One* 12(3):e0172999. <https://doi.org/10.1371/journal.pone.0172999>
 64. Leth-Espensen A, Glarborg P, Jensen PA (2018) Predicting biomass char yield from high heating rate devolatilization using chemometrics. *Energy Fuel* 32(9):9572–9580. <https://doi.org/10.1021/acs.energyfuels.8b02073>
 65. Howaniec N, Smoliński A (2014) Influence of fuel blend ash components on steam co-gasification of coal and biomass – chemometric study. *Energy* 78:814–825. <https://doi.org/10.1016/j.energy.2014.10.076>
 66. Smoliński A, Howaniec N (2017) Chemometric modelling of experimental data on co-gasification of bituminous coal and biomass to hydrogen-rich gas. *Waste Biomass Valor* 8(5):1577–1586. <https://doi.org/10.1007/s12649-017-9850-z>
 67. Smoliński A, Howaniec N (2017) Analysis of porous structure parameters of biomass chars versus bituminous coal and lignite carbonized at high pressure and temperature—a chemometric study. *Energies* 10(10). <https://doi.org/10.3390/en10101457>
 68. Cempa M, Smoliński A (2017) Reactivity of chars gasified in a fixed bed reactor with the potential utilization of excess process heat. *J Sust Mining* 16(4):156–161. <https://doi.org/10.1016/j.jsm.2017.12.001>
 69. Venturini E, Vassura I, Agostini F, Pizzi A, Toscano G, Passarini F (2018) Effect of fuel quality classes on the emissions of a residential wood pellet stove. *Fuel* 211:269–277. <https://doi.org/10.1016/j.fuel.2017.09.017>
 70. Jeguirim M, Kraiem N, Lajili M, Guizani C, Zorpas A, Leva Y, Michelin L, Josien L, Limousy L (2017) The relationship between mineral contents, particle matter and bottom ash distribution during pellet combustion: molar balance and chemometric analysis. *Environ Sci Pollut Res* 24(11):9927–9939. <https://doi.org/10.1007/s11356-017-8781-3>
 71. Schwabl M, Feldmeier S, Nagelhofer K, Wopienka E, Haslinger W. Applicability and slag formation survey of different biomass fuel qualities in small scale combustion: a substudy in the EU FP7-SME Project Ashmelt. In: *ETA-Florence Renewable Energies (Hg.) 2012 – Proceedings of the 20th European Biomass Conference and Exhibition*, pp 1156–1159
 72. European Pellet Council (2015) *ENplus Handbook: Quality Certification Scheme For Wood Pellets*
 73. Deutsches Institut für Normung (2011) *DIN EN 14780: Solid biofuels - Sample preparation*
 74. Deutsches Institut für Normung (2011) *DIN EN 14778: Solid biofuels - Sampling*
 75. Deutsches Institut für Normung (2014) *DIN EN ISO 17225-1: Solid biofuels - Fuel specifications and classes - Part 1: General requirements*
 76. Deutsches Institut für Normung (2003) *DIN EN 12457-4: Characterization of waste - Leaching; Compliance test for leaching of granular waste materials and sludges - Part 4: One stage batch test at a liquid to solid ratio of 10 l/kg for materials with particle size below 10 mm (without or with limited size reduction)*
 77. Retschitzegger S, Gruber T, Brunner T, Oberberger I (2015) Short term online corrosion measurements in biomass fired boilers. Part 1: application of a newly developed mass loss probe. *Fuel Process Technol* 137:148–156. <https://doi.org/10.1016/j.fuproc.2015.03.026>
 78. Panchuk V, Yaroshenko I, Legin A, Semenov V, Kirsanov D (2018) Application of chemometric methods to XRF-data – a tutorial review. *Anal Chim Acta* 1040:19–32. <https://doi.org/10.1016/j.aca.2018.05.023>
 79. Bro R, Smilde AK (2014) Principal component analysis. *Anal Methods* 6(9):2812–2831. <https://doi.org/10.1039/C3AY41907J>
 80. Jolliffe IT, Cadima J (2016) Principal component analysis: a review and recent developments. *Philosophical transactions. Series a, mathematical, physical, and engineering sciences* 374(2065):20150202. <https://doi.org/10.1098/rsta.2015.0202>
 81. Kumar K (2017) Principal component analysis: most favourite tool in chemometrics. *Resonance* 22(8):747–759. <https://doi.org/10.1007/s12045-017-0523-9>
 82. Mack R, Kuptz D, Schön C, Hartmann H (2019) Combustion behavior and slagging tendencies of kaolin additivated agricultural pellets and of wood-straw pellet blends in a small-scale boiler.

- Biomass Bioenergy 125:50–62. <https://doi.org/10.1016/j.biombioe.2019.04.003>
83. Deutsches Institut für Normung (2006) DIN CEN/TS 15370–1: Solid biofuels - Method for the determination of ash melting behaviour - Part 1: Characteristic temperatures method
 84. Björkman E, Strömberg B (1997) Release of chlorine from biomass at pyrolysis and gasification conditions 1. *Energy Fuel* 11(5):1026–1032. <https://doi.org/10.1021/ef970031o>
 85. Olsson JG, Jäglid U, Pettersson JBC, Hald P (1997) Alkali metal emission during pyrolysis of biomass. *Energy Fuel* 11(4):779–784. <https://doi.org/10.1021/ef960096b>
 86. Dayton DC, Jenkins BM, Tum SQ, Bakker RR, Williams RB, Belle-Oudry D, Hill LM (1999) Release of inorganic constituents from leached biomass during thermal conversion. *Energy Fuel* 13(4):860–870. <https://doi.org/10.1021/ef980256e>
 87. Dayton DC, French RJ, Milne TA (1995) Direct observation of alkali vapor release during biomass combustion and gasification. 1. Application of molecular beam/mass spectrometry to switch-grass combustion. *Energy Fuel* 9(5):855–865. <https://doi.org/10.1021/ef00053a018>
 88. Davidsson KO, Stojkova BJ, Pettersson JBC (2002) Alkali emission from Birchwood particles during rapid pyrolysis. *Energy Fuel* 16(5):1033–1039. <https://doi.org/10.1021/ef010257y>
 89. Jensen PA, Frandsen FJ, Dam-Johansen K, Sander B (2000) Experimental investigation of the transformation and release to gas phase of potassium and chlorine during straw pyrolysis. *Energy Fuel* 14(6):1280–1285. <https://doi.org/10.1021/ef000104v>
 90. Enders M, Willenborg W, Albrecht J, Putnis A (2000) Alkali retention in hot coal slag under controlled oxidizing gas atmospheres (air–CO₂). *Fuel Process Technol* 68(1):57–73. [https://doi.org/10.1016/S0378-3820\(00\)00110-7](https://doi.org/10.1016/S0378-3820(00)00110-7)
 91. Thy P, Leshner CE, Jenkins BM (2000) Experimental determination of high-temperature elemental losses from biomass slag. *Fuel* 79(6):693–700. [https://doi.org/10.1016/S0016-2361\(99\)00195-7](https://doi.org/10.1016/S0016-2361(99)00195-7)
 92. Wang Y, Wu H, Sárossy Z, Dong C, Glarborg P (2017) Release and transformation of chlorine and potassium during pyrolysis of KCl doped biomass. *Fuel* 197:422–432. <https://doi.org/10.1016/j.fuel.2017.02.046>
 93. Thy P, Jenkins BM, Grundvig S, Shiraki R, Leshner CE (2006) High temperature elemental losses and mineralogical changes in common biomass ashes. *Fuel* 85(5–6):783–795. <https://doi.org/10.1016/j.fuel.2005.08.020>
 94. Evic N, Brunner T, Obernberger I (2012) Prediction of biomass ash melting behaviour - correlation between the data obtained from thermodynamic equilibrium calculations and simultaneous thermal analysis (STA). In: *ETA-Florence renewable energies (ed) proceedings of the 20th European biomass conference and exhibition*, pp 807–813
 95. Li QH, Zhang YG, Meng AH, Li L, Li GX (2013) Study on ash fusion temperature using original and simulated biomass ashes. *Fuel Process Technol* 107(Supplement C):107–112. <https://doi.org/10.1016/j.fuproc.2012.08.012>
 96. Luan C, You C, Zhang D (2014) Composition and sintering characteristics of ashes from co-firing of coal and biomass in a laboratory-scale drop tube furnace. *Energy* 69:562–570. <https://doi.org/10.1016/j.energy.2014.03.050>
 97. Wang G, Jensen PA, Wu H, Frandsen FJ, Sander B, Glarborg P (2018) Potassium capture by kaolin, part 1: KOH. *Energy Fuel* 32(2):1851–1862. <https://doi.org/10.1021/acs.energyfuels.7b03645>
 98. Wang G, Jensen PA, Wu H, Frandsen FJ, Sander B, Glarborg P (2018) Potassium capture by kaolin, part 2: K₂CO₃, KCl and K₂SO₄. *Energy Fuel* 32:3566–3578. <https://doi.org/10.1021/acs.energyfuels.7b04055>
 99. Steenari B-M, Lindqvist O (1998) High-temperature reactions of straw ash and the anti-sintering additives kaolin and dolomite. *Biomass Bioenergy* 14(1):67–76. [https://doi.org/10.1016/S0961-9534\(97\)00035-4](https://doi.org/10.1016/S0961-9534(97)00035-4)
 100. Gilbe C, Öhman M, Lindström E, Boström D, Backman R, Samuelsson R, Burvall J (2008) Slagging characteristics during residential combustion of biomass pellets. *Energy Fuel* 22(5):3536–3543. <https://doi.org/10.1021/ef800087x>
 101. Olanders B, Steenari B-M (1995) Characterization of ashes from wood and straw. *Biomass Bioenergy* 8(2):105–115. [https://doi.org/10.1016/0961-9534\(95\)00004-Q](https://doi.org/10.1016/0961-9534(95)00004-Q)
 102. Fagerström J, Näzelius I-L, Gilbe C, Boström D, Öhman M, Boman C (2014) Influence of peat ash composition on particle emissions and slag formation in biomass grate co-combustion. *Energy Fuel* 28(5):3403–3411. <https://doi.org/10.1021/ef4023543>
 103. Johansen JM, Aho M, Paakkinen K, Taipale R, Egsgaard H, Jakobsen JG, Frandsen FJ, Glarborg P (2013) Release of K, Cl, and S during combustion and co-combustion with wood of high-chlorine biomass in bench and pilot scale fuel beds. *Proc Combust Inst* 34(2):2363–2372. <https://doi.org/10.1016/j.proci.2012.07.025>
 104. van Lith SC, Jensen PA, Frandsen FJ, Glarborg P (2008) Release to the gas phase of inorganic elements during wood combustion. Part 2: influence of fuel composition. *Energy Fuel* 22(3):1598–1609. <https://doi.org/10.1021/ef060613i>
 105. Sommersacher P, Kienzl N, Brunner T, Obernberger I (2016) Simultaneous online determination of S, Cl, K, Na, Zn, and Pb release from a single particle during biomass combustion. Part 2: results from test runs with spruce and straw pellets. *Energy Fuel* 30(4):3428–3440. <https://doi.org/10.1021/acs.energyfuels.5b02766>
 106. Näzelius I-L, Fagerström J, Boman C, Boström D, Öhman M (2015) Slagging in fixed-bed combustion of phosphorus-poor biomass: critical ash-forming processes and compositions. *Energy Fuel* 29(2):894–908. <https://doi.org/10.1021/ef502531m>
 107. Magdziarz A, Gajek M, Nowak-Woźny D, Wilk M (2018) Mineral phase transformation of biomass ashes – experimental and thermochemical calculations. *Renew Energy* 128:446–459. <https://doi.org/10.1016/j.renene.2017.05.057>
 108. Kaknics J, Defoort F, Poirier J (2015) Inorganic phase transformation in *Miscanthus* ash. *Energy Fuel* 29(10):6433–6442. <https://doi.org/10.1021/acs.energyfuels.5b01189>

Publisher's note Springer Nature remains neutral with regard to jurisdictional claims in published maps and institutional affiliations.